

**UNCLASSIFIED**

---

**AD 296 417**

*Reproduced  
by the*

**ARMED SERVICES TECHNICAL INFORMATION AGENCY  
ARLINGTON HALL STATION  
ARLINGTON 12, VIRGINIA**



---

**UNCLASSIFIED**

7

NOTICE: When government or other drawings, specifications or other data are used for any purpose other than in connection with a definitely related government procurement operation, the U. S. Government thereby incurs no responsibility, nor any obligation whatsoever; and the fact that the Government may have formulated, furnished, or in any way supplied the said drawings, specifications, or other data is not to be regarded by implication or otherwise as in any manner licensing the holder or any other person or corporation, or conveying any rights or permission to manufacture, use or sell any patented invention that may in any way be related thereto.

63-2-4

CATALOGED BY ASTIA 29 6417



COPY NO. 10

PICATINNY ARSENAL TECHNICAL REPORT 3063

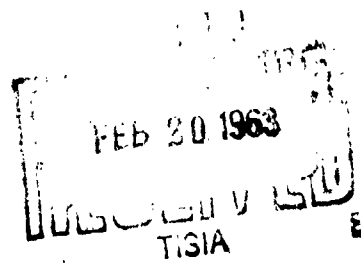
THE COMBUSTION OF A GRANULAR MIXTURE  
OF POTASSIUM PERCHLORATE AND ALUMINUM  
CONSIDERED AS EITHER A DEFLAGRATION  
OR A DETONATION

JOSEPH HERSHKOWITZ

JANUARY 1963

PICATINNY ARSENAL  
DOVER, NEW JERSEY

296 417



The findings in this report are not to be construed as an official Department of the Army position.

#### DISPOSITION

Destroy this report when it is no longer needed.  
Do not return.

#### ASTIA AVAILABILITY NOTICE

Qualified requesters may obtain copies of this report from ASTIA.

**THE COMBUSTION OF A GRANULAR MIXTURE OF  
POTASSIUM PERCHLORATE AND ALUMINUM CONSIDERED AS  
EITHER A DEFLAGRATION OR A DETONATION**

by

**Joseph Hershkowitz**

**January 1963**

**Feltman Research Laboratories  
Picatinny Arsenal  
Dover, New Jersey**

**Technical Report 3063**

**OMS 5010.11.815009**

**DA Project 5030-4002**

Approved by

*W R Benson*

**W. R. BENSON  
Chief, Engineering  
Sciences Laboratory**

## TABLE OF CONTENTS

	Page No.
ABSTRACT	1
INTRODUCTION	2
DIFFUSIVITY CONSIDERATIONS	3
Molecular Diffusion	5
Thermal Diffusion	5
Radiant Energy Diffusion	6
SOUND SPEED CONSIDERATIONS	7
Assumptions and Definitions	7
Dusty Gas	10
Porous Elastic Solid	10
Loosely Packed Granular Aggregate	11
Discussion of Sound Speed Results	14
ONE-PARAMETER HYDRODYNAMIC COMBUSTION THEORY	15
Basic Assumptions and Equations	15
Numerical Results and Discussion	20
CHAPMAN-JOUGUET DETONATION CONSIDERATIONS	21
Inputs and Parametric Studies	21
Numerical Results	23
OVERALL DISCUSSION	24
Further Experimental Work	24
Further Theoretical Work	25
ACKNOWLEDGEMENTS	26
REFERENCES	27

<b>TABLE OF CONTENTS (Continued)</b>		
<b>TABLES</b>		<b>Page No.</b>
1	Data on the Compression of Aluminum Powder	33
2	Sound Speed Results for the Granular Aggregate Model	35
3	One Parameter Hydrodynamic Combustion Theory Results	36
4	Tentative Hugoniot Data for Aluminum Oxide	37
5	RUBY Input Data	38
6	Results of RUBY Runs	41
<b>FIGURES</b>		
1	Propagation of Combustion in the Granular Mixture	43
2	Two Reaction Zone Profiles	44
3	Sound Speed Considerations	45
<b>APPENDICES</b>		
A	Derivation of the Jump Conditions by Two Approaches	
B	Solution of the Equations of the One Parameter Hydrodynamic Combustion Theory	
<b>INITIAL DISTRIBUTION LIST</b>		i

## ABSTRACT

The combustion front in a column of a granular mixture of potassium perchlorate and aluminum has been observed to propagate stably at either a low speed (300 m/s) with a short reaction zone (2 cm), or a high one (900 m/s) with an elongated reaction zone (8 cm), and with an occasional rapid transition between them. Calculations are made to categorize the observed phenomena as those of either a deflagration or a detonation.

Calculating the penetration depth from the front into the mixture for diffusion of molecules, thermal energy, and radiant energy shows that these deflagrative mechanisms have negligible effect at the rates observed and suggests that deflagration would proceed at less than 0.3 m/s. A calculation of the deflagration branch of the Hugoniot by a parametric technique also shows that only rates of the order of 0.1 m/s exist for deflagrations. The calculated sound speed for the unreacted granular mixture is less than 300 m/s. The hypotheses of a simple deflagration and of a deflagration following a precompression shock are rejected.

The RUBY computer program calculated a detonation velocity for the mixture of 4600 m/s. This would be reduced by the observed lateral rarefaction in the reaction zone. It is concluded that to establish the details of the detonative nature of the phenomena further experiments are required on effect of confinement, interstitial gases, diameter and length of mixture column, and time-resolved spectroscopy of the reaction zone structure. Future theoretical consideration should either combine the physical kinetics of aluminum particle vaporization with a two-phase theory or examine coupling between shock and combustion within the reaction zone.



## INTRODUCTION

This report explores the nature of the combustion wave in a granular mixture of potassium perchlorate and aluminum. The mixture is a powder, which, when loose-loaded into a case and initiated by an imbedded small explosive, produces a short, intense flash of light. Several years ago, research was started on the physics of these photoflash items. The first phase (Ref 1) of the research showed by means of flash radiographs that a small PETN charge centered in nonreacting metal dust (simulating mechanical properties of the mixture) formed an expanding bubble of explosion products surrounded by an ever-thickening spherical shell of compressed metal dust. This behavior was also described theoretically.

The nonreacting metal dust was then replaced by the potassium perchlorate/aluminum mixture and its interaction with the confining case was studied in relation to the light output and the size of the cloud that is formed from the item (Ref 2).

Theoretical treatment requires information on the combustion process that occurs in the confined mixture under explosive initiation. The next phase (Refs 3, 4) was therefore devoted to gathering information on combustion rates. The experimental approach used was to confine the mixture along the axis of a thick cylinder of transparent plastic and then use high speed photographic techniques to observe the propagation of combustion after initiation by an explosive located at one end of the mixture column. The results obtained were more complicated than anticipated.

In Figure 1, successive stages in one type of combustion are shown, as viewed initially by backlighting and later only by emitted light. The upper left photo shows a transparent plastic rod 3 inches in diameter and 20 inches long, with a 3/8-inch-diameter column of loose-loaded mixture along the axis. The notches in the supporting bar are 1 inch apart. Initiation occurred at the left. The photos shown are 96 microseconds apart. The lower right photo is the stable reaction zone profile that is observed to move at about 900 meters per second. Note that the highly luminous region extends forward into the mixture column and that there follows a dark area preceding a luminous cloud.

In some cases a different stable profile is observed propagating at only about 300 meters per second, with no such forward extension, or dark zone and following cloud. This slower profile, a small, bright

region surrounded by a much larger, less luminous cloud, is shown in Figure 2 together with the type described above. In addition a rapid transition (almost always to the higher speed) between the two stable states was occasionally observed. By both necessity and interest, the research since then has been concerned with explaining the essential features of these experimental results.

The following possibilities were previously considered qualitatively (Ref 4) high-speed deflagration; deflagration with a precompression shock; deflagration preceded by an interstitial detonation (the latter involves only the fines suspended in the interstices of the powder); or a detonation with an expanded reaction zone associated with the chemical and physical kinetics of the medium. This report begins a quantitative treatment by providing calculations on diffusion of molecular species and energy, sound speeds possible in the medium, the deflagration branch of the Hugoniot curve, and the Chapman-Jouguet values for a detonation. In each case the significance of the results is discussed in determining the mechanism involved in the propagation of the combustion. Directions for future experimental and theoretical studies are then proposed.

It will be assumed in the treatment that follows that the reader has some familiarity with deflagrative and detonative combustion theories (Ref 5, 6) and other related subjects. However, adequate information will be supplied on the physical significance of the equations used, to permit following the logic of the presentation.

## DIFFUSIVITY CONSIDERATIONS

A deflagration is a form of combustion in which the flame progresses by diffusion of both activating species and energy from the reaction zone into the unreacted mixture. The classical partial differential equation (Ref 7) that governs this process is (for one dimension, constant  $\chi$ , no sources)

$$\chi \frac{\partial^2 T}{\partial x^2} = \frac{\partial T}{\partial t} \quad (1)$$

Where  $T$  is the temperature for energy flow or the concentration for flow of molecular species.  $\chi$  is a constant called the diffusivity, which from the equation has the dimensions of length squared divided by time, or of velocity times length.

For our case, we replace the combustion wave which proceeds at a constant velocity  $U$ , maintaining the same profile, by a model having energy release in a fixed plane at  $x = 0$ , preheating the region in front of this plane which moves with speed  $-U$  (to the left) toward it. At and behind the plane ( $x = 0$ ) a fixed temperature or concentration ( $T_0$ ) is assumed. Although the model can be made more sophisticated, it is not necessary to do so for the order of magnitude results required. We rewrite equation 1 as

$$x \frac{d^2 T}{dx^2} = - \frac{dT}{dx} U \quad (1a)$$

Solving equation 1a subject to the boundary conditions that  $x \leq 0$   $T = T_0$ ;  $x \rightarrow \infty$   $T \rightarrow \infty$  one finds for  $x > 0$  (the region that is preheated)

$$\frac{T - T_\infty}{T_0 - T_\infty} = e^{-\frac{U}{\kappa} x} \quad (2)$$

and energy flux =  $\rho c_p U (T_0 - T_\infty) e^{-\frac{U}{\kappa} x}$

The temperature and flux decay to  $1/e$  of the value at  $x = 0$  as one moves a penetration distance,  $L$ , to the right ( $x > 0$ ), where

$$L = \frac{\kappa}{U} \quad (3)$$

This result corresponds to the dimensional result following equation 1. The penetration distance is the length of unreacted mixture directly in front of the flame front into which energy and molecular species can penetrate to initiate chemical reaction. It is shown later that the values of  $L$  from equation 3 are about 1 micron.

For the flame front to continue to move forward with the same profile at a speed of  $U$ , the energy release from the flame front into the penetration length would have to occur in a time  $t = L/U$ . For  $U = 300$  m/s,  $L = 1$  microm,  $t = 3.3 \times 10^{-9}$  seconds results. However, a separate calculation shows that the 15-micron-diameter aluminum granule requires of the order of  $10^{-7}$  second to liquefy and  $10^{-5}$  second to fully vaporize under optimum conditions of continuous exposure to the flame temperature. Since the energy can not be released except in proportion to aluminum vaporized, one must conclude, since  $10^{-5} \gg 10^{-9}$ , that a deflagration propagated by these mechanisms at 300 m/s cannot exist in this mixture.

Note that if particle sizes were reduced to sub-micron dimensions so that vaporization were orders of magnitude faster, the arguments advanced would not be valid. This will be used in the later discussion of interstitial effects.

To contrast with the fact that a deflagration at 300 m/s in this mixture is not possible, consider the possibility of one at 0.3 m/s. Using equation 3, it follows that now the penetration length, call it  $L_1$  will be  $10^3$  greater than the penetration length for 300 m/s; thus  $L_1$  is of the order of  $10^3$  micron. Then  $t_1 = \frac{L_1}{U_1} = 3.3 \times 10^{-3}$  seconds. These values of  $L_1$  and  $t_1$  indicate, since  $10^{-5} \ll 10^{-3}$ , that a reasonable speed for deflagration if it existed would be about 0.3 m/s or less.

The above presentation has used the fact that  $L$  computed from equation 3 is of the order of 1 micron. The values of  $L$  are derived below and substantiate the conclusions of the previous paragraphs.

#### Molecular Diffusion

Chemical reaction can be initiated by molecular species, present in the flame zone, moving into the unreacted mixture. The concentration of these activating species will be established by diffusion. Typical values (Ref 8) of diffusivity ( $\text{cm}^2/\text{sec}$ ) for gases into air at 1 atm and about  $20^\circ\text{C}$  are, for  $\text{CO}_2$ ,  $\text{O}_2$ , and  $\text{H}_2\text{O}$  vapor, 0.139, 0.178, and 0.239 respectively. For dilute gas binary mixtures (Ref 9) diffusivity decreases inversely with pressure and increases roughly as the 1.8 power of temperature. The flame temperature is estimated as  $3000^\circ\text{K}$  and the pressure therein should be less than atmospheric. However, the unreacted mixture is at room temperature and atmospheric pressure (except for the effect of simultaneous energy diffusion considered below).

For estimating purposes, one can use  $X = 0.2$ , subject to a maximum increase due to temperature of 63 times, that is,  $(3000/300)^{1.8}$ . The lowest observed flame velocity was  $3 \times 10^4 \text{ cm/s}$ . The penetration distance  $L = 0.2/(3 \times 10^4) = 0.066$  micron, which, even if multiplied by 63, is only about 4 microns.

#### Thermal Diffusion

The approach is similar to that above. For aluminum particles the

thermal diffusivity (Ref 8) is about 1.35 and for air it is 0.16. Using the larger value and equation 3 we find  $L = 0.45$  micron.

### Radiant Energy Diffusion

The key assumption made in this case is that thermal equilibrium exists between radiation and the granular media. One can then use (Ref 10) the equilibrium (black body) relationships to show that the radiative flux is related to the temperature distribution by

$$q_R = -\frac{4}{3} a c \lambda_R T^3 \frac{dT}{dx} = -k_R \frac{dT}{dx} \quad (4)$$

Here  $k_R$  is radiation conductivity analogous to thermal conductivity. Defining a radiation diffusivity  $\chi_R = k_R / \rho c_p$  and using equation 3 we find a penetration distance

$$L = \frac{4}{3} \frac{a c \lambda_R T^3}{\rho c_p U} \approx \frac{\lambda_R}{30} \text{ for } U = 300 \text{ m/s } T = 3500^\circ \text{K} \quad (5a)$$

$$\approx 30 \lambda_R \text{ for } U = 0.3 \text{ m/s } T = 3500^\circ \text{K} \quad (5b)$$

where  $a$  is the Stefan Boltzmann constant ( $7.67 \times 10^{-15}$  ergs/cm<sup>3</sup> deg<sup>4</sup>),  $c$  the velocity of light ( $3 \times 10^{10}$  cm/sec),  $\rho$  the density of air (0.00125 gms/cm<sup>3</sup>),  $c_p$  the specific heat of air (0.285 cal/g), and  $\lambda_R$  the Rosseland mean free path, which is essentially the photon mean free path.

Microphotographs (Ref 1) of granular media at this loading density and particle size indicate that  $\lambda_R$  must be of the order of 30 microns, that is, twice the average particle size. One can interpret equation 5a as leading to a penetration distance for radiation by diffusion of only 1 micron. However, it is more instructive to compare equation 5a with 5b. For the latter, the result states that radiation will be absorbed and re-emitted over a length 30 times the mean free path of a photon ( $\lambda_R$ ) when energy is transmitted forward by radiation and both the flux and the local temperature associated therewith will fall to  $1/e$  of the maximum of a distance  $L$ . A value of  $L$  less than  $\lambda_R$  indicates that the basic process of absorption and re-emission has no significant role. This confirms the previous numerical analysis for all modes of diffusion based on the 1-micron length.

It follows that at the observed rates of 300 m/s or higher and maximum temperature of 3,500° K, radiation is not a significant factor.

### SOUND SPEED CONSIDERATIONS

The combustion front of a one-dimensional deflagration progresses at a rate that is subsonic with respect to the sound velocity in the unreacted medium (Ref 5) preceding it. For a deflagration preceded by a precompression shock, the shock is supersonic with respect to the medium it is entering, and the deflagration follows at a subsonic speed measured relative to the precompressed medium preceding it. A detonation front progresses at a supersonic rate with respect to the unreacted medium. Thus a comparison of the sound speed in the unreacted medium and that in a compressed medium with the experimentally observed propagation rate would establish the nature of the phenomenon under the assumption that it is one dimensional.

To consider these possibilities one requires data on the sound speeds in the granular medium as a function of density. Since applicable experimental data or theoretical results were not found in the literature (Refs 18-28) and experimental facilities for the measurements were not available, theoretical calculations as described below were used. The numerical results are shown in Figure 3. Their significance with respect to the observed combustion phenomena is treated in the later subsection entitled "Discussion of Sound Speed Results."

#### Assumptions and Definitions

In general, for a medium with no changes in chemical composition, the sound speed is defined by

$$c^2 = \left( \frac{\partial p}{\partial \rho} \right)_S \quad (6)$$

However, different sound speeds can exist depending on how the constant entropy condition is met. For a two-phase (gas and granules) flow this will depend on the relative motion of the two phases and the heat transfer between them during the period of the sound wave.

The equilibrium sound speed is defined as that in which only the total entropy is held constant. Since relative flow of gas with respect to

granules is a viscous flow, generating entropy, one must assume here that there is no significant relative motion during the period of the sound wave. This would be valid for the frequency low enough so that the time required to equalize velocities is a small fraction of the period. Further, since only the total entropy is held constant, heat transfer between the two phases is permissible if there is no generation of entropy. This will be the case if the transfer is quasistatic (i. e., takes place with infinitesimal temperature differences), which can be met only for sound waves with periods long compared to the time required for temperature equalization. To make quantitative estimates on how low the frequency of a sound wave must be for an equilibrium sound speed to exist, one would have to calculate the viscous relaxation time and the thermal relaxation time for the medium and make the period several times greater than either. For our immediate purpose, it is adequate to think of the equilibrium sound speed as that valid in the low frequency limit.

Next, we define two different frozen sound speeds in each of which we specify how the total entropy is maintained constant by imposing additional conditions. Consider that frozen sound speed (designated I) in which there is no heat flow and no relative motion between the two phases. The entropy of each phase is maintained constant separately and no entropy generation is permitted, so obviously the total will be constant. Physically, no heat transfer requires a high frequency sound wave (short period) so that no significant heat flow can occur. Velocity equalization has the opposite requirement of long periods. However, one can create some special cases where both conditions might be simultaneously satisfied. Suppose the medium is sufficiently compressed so that the aluminum granules form a lattice with pockets of gas almost totally enclosed by metal surfaces. A rapid compression of the lattice will transport the gas with very little relative motion and for such short times the heat transfer could be negligible also. The frozen sound speed (I) is therefore the high frequency limit for the porous lattice. However, for the granular aggregate model (to be defined later) there is no frozen sound speed (I) because there is always a generation of entropy due to friction as the granules move relative to each other, so that one cannot hold the total entropy and also that of the gas constant.

Another frozen sound speed (designated II) would also permit no temperature equalization, but would have the particles stationary during the gas motion. For sufficiently high frequencies the wavelength of the sound wave is a fraction of the particle size and the relative motion of the gas

with respect to the particles produces an insignificant quantity of entropy. This frozen sound speed (II) is the high frequency limit for the dusty gas model and the granular aggregate model (particles stationary), and will correspond with the ordinary sound speed in the gas alone.

It is to be noted that physically there are cases where the total entropy is not constant during the passage of a weak mechanical vibration or sound wave. The theoretical treatment must therefore calculate both the equilibrium and frozen sound speeds, which are the low and high frequency limits, respectively, and assume that the intermediate nondefinable cases represent velocities between them. This range is then used for comparison with the observed velocity of propagation of combustion to determine whether the latter is subsonic or supersonic.

Next, we consider assumptions on the nature of the medium. In the limit of low densities, the powder is a dusty gas. In fact before this lower limit is reached there may be small pockets of powder which act as a dusty gas. This is because a dusty gas is defined as one in which the particles do not participate directly in resisting the applied load. Particles may be in contact but if they are not under load, the medium is still called a dusty gas. In the limit of high densities, the powder is a porous elastic solid with a lattice formed by the particles and an interstitial compressible gas. In the range of densities between, there is a relative motion of particles forming successive load-sustaining geometrical configurations. This intermediate region is called the granular aggregate case and is believed to correspond most closely to the actual medium. It will be treated by using an experimentally determined stress-strain curve. The dusty gas and porous elastic solid limiting cases will also be considered.

In all cases, the medium is taken as consisting of aluminum granules only instead of as a mixture of aluminum and potassium perchlorate. The experimental curve used for the granular aggregate could only be safely determined for aluminum alone. The equations which will be used are derived only for a metal powder, and extending these to more than one solid component would involve considerable algebra. However, this assumption introduces no significant error because the difference between the mechanical properties of air as compared to those of either aluminum or potassium perchlorate is orders of magnitude greater than the difference between the mechanical properties of the two solids. For this reason the conclusions based on an aluminum dust are the same as would follow from



an extended consideration. This will be evident in the numerical treatments presented and will be discussed for the granular aggregate case.

#### Dusty Gas

For a dusty gas of rigid aluminum particles the equilibrium and frozen (I) sound speeds have been computed (Ref 11). The frozen (II) sound speed is approximately that for the gas alone. The numerical results are shown in Figure 3 for densities up to 1.1 g/cm<sup>3</sup>. The frozen (I) and equilibrium sound speeds were close enough to permit plotting only one curve to represent both. The frozen (II) sound speed is about 330 m/s by definition. Higher densities were not considered because the medium at 1.1 g/cm<sup>3</sup> is already beyond the dusty gas range, as shown by microphotographs of the powder. The density of the medium in the experiments was above 1.3 g/cm<sup>3</sup> showing that the dusty gas approximation is of limited value. It does help to show that as particles are added to a gas the mass loading causes the sound speed to rapidly decline, flattening out at a low value. The sound speed only increases when particle contacts sustain load and thus increase the elasticity of the medium.

#### Porous Elastic Solid

The analog to the frozen (II) sound speed in the dusty gas is the speed in the material of which the particles are composed. Just as in the dusty gas, there is some small quantity of energy that finds its way through a pure gas path, so for the porous elastic solid, there will be some energy transmitted through a purely solid path. In the latter, the frequency will have to be high enough so that there is no coupling to the interstitial gas. The frozen (II) sound velocity for an aluminum powder is therefore about 5180 m/s.

The equations for frozen (I) and equilibrium sound speed are (Ref 12)

$$c_f^2 = \gamma' \left( \frac{2\mu + \lambda + \frac{\beta^2 \tau_0}{\alpha'}}{\rho_0'} \right) + \gamma'' \left( \frac{\beta_0 \tau''}{\rho_0''} \right) \quad (7)$$

$$c^2 = \gamma' \left( \frac{2\mu + \lambda + \frac{\tau_0}{\alpha} (1-f_0) \beta^2}{\rho_0'} \right) + \gamma'' \left( \frac{\beta_0 \tau''}{\rho_0''} \right) + 2f_0 (1-f_0) \frac{\beta}{\alpha} \frac{\beta_0}{\rho_0} \quad (8)$$

For convenience, it has been assumed that the interstitial gas behaves like

a perfect gas and the elastic matrix behaves like a Hookian material. A single prime represents the solid, a double prime the air.  $Y$  is the mass fraction of the phase.  $f_0$  is the initial porosity defined as the fraction of the total volume occupied by the gas at  $p_0, T_0, p_0$ .  $\Delta$  is specific heat per unit volume (at constant volume).  $\mu$  and  $\lambda$  are Lamé's constants and  $\beta$  is the thermoelastic constant. These can (Refs 13, 14, 15) be related to common mechanical and thermal parameters such as bulk modulus and coefficient of thermal expansion. Numerical values are available (Ref 16).

Equation 7 states that the square of the frozen sound speed in the mixture is exactly equal to the mass fraction weighted mean of the square of the isentropic sound speeds in the elastic matrix and the interstitial gas. For the mixture  $Y' = 0.9995974$  and  $Y'' = 0.0004026$  and tabulated values for the sound speed in aluminum and air are 5182 m/s and 331 m/s. It follows that the frozen sound speed is about that of the solid of which the particles are composed. Thus both frozen sound speeds are about 5180 m/s for an aluminum powder. For a mixture of aluminum and potassium perchlorate there may be a narrow range of velocities determined by the properties of the two materials and the statistical distribution of paths for the sound energy.

Equation 8 was used to calculate the equilibrium sound speed for densities above 1.1 g/cm<sup>3</sup>. The results (shown in Figure 3) indicate that for densities above 1.1 the sound speed is approximately constant at 6400 m/s. The numerical value obtained is associated with the data used. The point to note is that even for a density as low as 1.1, a very high equilibrium sound velocity is calculated as soon as one uses the porous elastic medium approach.

#### Loosely Packed Granular Aggregate

Since the dusty gas and porous elastic solid approaches provide only extreme limits to the true nature of the medium, and give sound speeds so far apart, and bracketing the observed values, it becomes necessary to try and make a better calculation.

Let  $\sigma$  be the force per unit area applied to a piston of area  $A_p$  compressing unit mass of the mixture a distance  $dx$  ( $dV = A_p dx$ ), then  $\sigma = \sigma' + \sigma''$  where  $\sigma'$   $\sigma''$  are the forces per unit area of mixture supported by the granules and gas respectively. The equilibrium sound

speed is

$$c^2 = \left( \frac{\partial \sigma}{\partial \rho} \right)_{S_0} = -V^2 \left( \frac{\partial \sigma}{\partial V} \right)_{S_0} = -V^2 \left[ \left( \frac{\partial \sigma'}{\partial V} \right)_{S_0} + \left( \frac{\partial \sigma''}{\partial V} \right)_{S_0} \right] \quad (9)$$

where  $S_0$  is the total entropy at  $T = T_0$ ,  $V = V_0$  specific volume for the mixture.

If  $V_0$ ,  $V_0'$  are the initial volumes per unit mass of the mixture occupied by the mixture and granules respectively, at temperature  $T_0$ , then

$$\sigma' = F \left( \frac{V_0 - V}{V_0}, T - T_0 \right) \quad (10)$$

where  $F$  is a function to be determined. Write  $F_0$  for  $F$  with  $T = T_0$ . Now  $F_0$  has been measured (Ref 1) by compressing aluminum powder so slowly that the interstitial gas remained in pressure equilibrium with the atmosphere and an isothermal condition was achieved at the temperature,  $T_0$ , of the compression device, for the mixture. The results are plotted in Reference 1 and given here in Table 1 together with least square fits for  $\rho \geq 1.4$ .

The role of temperature in equation 10 is assumed to be primarily that of changing the size of the granules and so increasing the stress with temperature. This assumption is reasonable for densities above 1.4 g/cm<sup>3</sup>. An increment  $dT$  will increase the stress by  $d\sigma'$  the amount required to recompress the mixture to the volume that existed prior to raising the temperature.

$$d\sigma' = \frac{dF_0}{d\left(\frac{V_0 - V}{V_0}\right)} \frac{d\left(\frac{V_0 - V}{V_0}\right)}{d(T - T_0)} d(T - T_0) = - \frac{dF_0}{d\left(\frac{V_0 - V}{V_0}\right)} \frac{V_0'}{V_0} \alpha' dT \quad (11)$$

Where  $\alpha' dT = \frac{\alpha \tau'}{\tau_0}$  with  $\alpha'$  the coefficient of thermal expansion of aluminum and  $\tau_0'$ ,  $\tau'$  the specific volumes of aluminum at  $T_0$ ,  $T$  respectively. In deriving the above  $\alpha \tau' = 0$  and  $\alpha V'' \approx 0$  have been used as characterizing a granule thermal expansion with restoration to same mixture volume by increase in applied load. Using a constant coefficient of thermal expansion  $\alpha'$ , and integrating from  $T_0$  to  $T$ , one finds

$$\sigma' = F_0 \left( \frac{V_0 - V}{V_0} \right) - \frac{\alpha' (T - T_0) V_0'}{V_0} \frac{dF_0}{d\left(\frac{V_0 - V}{V_0}\right)} \quad (12)$$

For  $\sigma''$  in equation 9 we can use the perfect gas law

$$\sigma'' = \frac{RT}{V - V'} \quad (13)$$

where  $V'$  is the volume occupied by the granules.

It can be shown (Ref 17) that the entropy of the mixture is

$$S - S_0 = R \ln \left( \frac{V - V'}{V_0 - V'} \right) - \left( \frac{d\alpha}{dT} - \frac{d\alpha}{dT} \Big|_{T_0} \right) \quad (14)$$

$$\text{where } \alpha(T) = A_0 \frac{T - T_0}{T_0} - T \int_{T_0}^T \frac{U(T)}{T^2} dT \quad (15)$$

If in equation 15 we use  $U' = c_v' T$   $U'' = c_v'' T$  and define  $c_v = Y' c_v' + Y'' c_v''$  so that  $U = c_v T$  and substitute in equation 14, we find the condition for  $S = S_0$  is

$$\frac{T}{T_0} = \left[ \frac{V - V'}{V_0 - V'} \right]^{-R/c_v} = g \quad (16)$$

Equation 16 is used in equations 12 and 13. These are then differentiated and used in equation 9 to find the equilibrium sound speed. However, equations 13 and 16 both contain  $V'$ . It is assumed that  $V' \approx V_0'$  where  $V_0'$  is the initial volume occupied by the granules. The justification is that the principal mechanism in the deformation range considered is rearrangement of granules from one load-sustaining structure to another. The density range for this to be valid is estimated as  $1.4 \leq \rho \leq 1.9$

The final result for the equilibrium sound speed is then

$$c^2 = V^2 \left( \frac{F_0'}{V_0} + \alpha' V_0' T_0 \frac{F_0''}{V_0^2} \right) - \frac{\alpha' V_0' V^2 T_0 g}{V_0} \left[ \frac{F_0' R}{c_v (V - V_0')} + \frac{F_0''}{V_0} \right] + \frac{g R T_0 V^2}{(V - V_0')^2} \left( \frac{R}{c_v} + 1 \right) \quad (17)$$

The results of calculation with this formula are given in Table 2 and plotted in Figure 3. As the density is lowered from 1.45 the sound speed

7

drops rapidly toward the dusty gas range. This drop represents a decrease in the number of load-bearing granule contacts. As the density increases beyond  $\rho = 1.6$  the sound speed rises slowly as granular structure rearrangements occur. One expects that at some density near that of aluminum ( $\rho = 2.7$ ) the structure will become locked and the sound speed will simultaneously rise rapidly to that of the porous elastic solid model.

#### Discussion of Sound Speed Results

In the introduction to this Sound Speed Considerations section, it was observed that to determine whether the observed combustion propagated subsonically or supersonically one required sound speed data. Figure 3 summarizes the results of the calculations and also shows the range of speeds observed for propagation of combustion in the mixture. The latter are obviously supersonic, leading to the conclusion that the observed propagation of combustion is not a simple deflagration. For a deflagration preceded by a precompression shock, the deflagration would have to be subsonic with respect to the precompressed medium. Suppose a density change from 1.5 to 1.8 across the shock, then by conservation of mass the compressed mixture directly behind the shock will be moving in the same direction at  $(1 - \frac{1.5}{1.8})$  times the shock velocity. For a shock at 900 m/s, the medium will be traveling at 750 m/s. The deflagration would have to travel at 900 m/s relative to the observer to maintain a stable profile. However, this requires the deflagration to travel at 750 m/s relative to the compressed medium. From the sound speed results at  $\rho = 1.8$ , this is not subsonic as required. Therefore, the higher speed, elongated, stable profile can not be a deflagration with a precompression shock. This leads to the conclusion that all the observed propagation of combustion is detonative, which is the same as the conclusion reached by means of the diffusivity considerations. There were sufficient assumptions (e. g. metal dust representing the mixture) made in the sound speed calculations to raise some doubt as to the confidence to be placed solely in the absolute values of the sound speed results. However, they are only being used as one indicator in the analysis of the observed phenomena. In the next section, still another approach is used to examine the nature of the observed propagation of combustion.

## ONE-PARAMETER HYDRODYNAMIC COMBUSTION THEORY

A direct approach to determining whether the experimental results represent a deflagration is to calculate the speed that a deflagration front would have in this particular mixture. However, available theories (Refs 29, 30) must assume a reaction rate law to provide a complete set of equations. (For a detonation, the Chapman-Jouguet stability condition is available.) Introducing this assumption, which limits the validity of the results (Ref 30), is not necessary for the purpose at hand. If the entire deflagration branch of the Hugoniot could be shown to lead to no propagation velocity comparable with that observed experimentally, then it would have been proven that the observed combustion was not a deflagration. The one-parameter hydrodynamic combustion theory (OPHCT) which is developed in this report calculates the deflagration branch of the Hugoniot using the downstream temperature as a parameter. Other features of the Hugoniot such as the dead zone and a detonation branch of limited validity are also developed. In agreement with the diffusivity and sound speed results, it is found that the experimental observations can not be explained as a deflagration. In the remainder of this section the OPHCT is developed. The next section then considers the detonation possibility.

### Basic Assumptions and Equations

We shall immediately assume the following:

- a. All upstream constituents are consumed in the chemical reaction; that is, combustion is complete.
- b. No external heat losses or external work need be considered; that is, the problem is one dimensional.
- c. A steady state exists as viewed by an observer traveling with the flame front; that is, there is a constant reaction zone profile traveling at constant speed.
- d. The decomposition and interaction of K Cl can be neglected.
- e. The temperature up to the Chapman-Jouguet plane is above 2800° K so that it can be assumed that liquid Al is not present.
- f. The species chosen as products are the significant ones.

$\text{Al}_2\text{O}_2$ ,  $\text{Al Cl}_3$ , and  $\text{Al}_2\text{O}_3(\text{g})$  are omitted.

g. An appropriate equation of state is that for a perfect gas with the volume occupied by condensed phase  $\text{Al}_2\text{O}_3$  subtracted out. The equation of state of condensed  $\text{Al}_2\text{O}_3$  is ignored.

Assumption a avoids the possibility that some of the aluminum is not consumed, which would introduce a second parameter and require consideration of the thermal energy sink action (Ref 31) of the unconsumed particles. Since full consumption of the aluminum will lead to the highest propagation rate, assumption a was justified.

Assumptions b and c make the problem an algebraic one by permitting use of the discontinuous solutions (jump conditions) of the differential equations representing conservation of mass, momentum, and energy. Appendix A derives the jump conditions in a manner which shows that assumption c is needed for a finite thickness flame zone.

Assumptions d, e, and f are of the type one must always make in combustion calculations; i.e. one must choose the products. These choices were guided by experience in the aluminized propellant field since the primary interest was in deflagrations (low pressures). In fact, these choices serve to invalidate the calculation of the detonation branch by the OPHCT because, as will be evident in the detonation section of this report, other products must be assumed for the high pressures of detonation.

Assumption g is again valid for the low pressures of deflagrations and invalid for the detonation branch where one must use an equation of state suitable for high pressures (Ref 32).

Next we state the applicable equations.

Let  $U$  be the velocity, positive to the right of the combustion zone. Then if  $u_1$  and  $u_2$  are the particle velocities upstream and downstream within the stable reaction zone profile, and  $v_1$  and  $v_2$  are the same relative to the combustion zone, we have  $v_1 = u_1 - U = -U$  since  $u_1 = 0$  and  $v_2 = u_2 - U$ .

Following a mass element in the flow, the jump conditions (Rankine-Hugoniot) as derived in Appendix A are, for the conservation of mass

$$\rho_1 v_1 = \rho_2 v_2 \quad (18)$$

for conservation of momentum

$$\rho_1 v_1^2 + p_1 = \rho_2 v_2^2 + p_2 \quad (19)$$

for the conservation of energy

$$h_1 + \frac{1}{2} v_1^2 = h_2 + \frac{1}{2} v_2^2 \quad (20)$$

These can be combined into the Hugoniot Adiabatic Equation

$$h_2 - h_1 = \frac{1}{2} (p_2 - p_1) \left( \frac{1}{\rho_1} + \frac{1}{\rho_2} \right) \quad (21)$$

which replaces the energy equation.

Here  $h_1$  and  $h_2$  are functions of both the temperature and composition, and under certain assumptions could also depend on the pressure.

A fourth equation that applies is the equation of state, which, if one considers the volume occupied by the condensed  $\text{Al}_2\text{O}_3$ , becomes the following modification of the perfect gas law.

$$\frac{1}{\rho_2} = \frac{R_m T_2}{p_2} \frac{1}{\sum' x_i m_i} + \frac{1}{\rho_{\text{Al}_2\text{O}_3}} \frac{x_{\text{Al}_2\text{O}_3} m_{\text{Al}_2\text{O}_3}}{\sum' x_i m_i} \quad (22)$$

The  $\sum'$  indicates a summation over all species, whereas  $\sum$  is used for gaseous species only. The  $x_i$  and  $m_i$  are the mole fraction and molecular weight respectively. Using the same notation, the enthalpy of the product mixture used in equation 21 can be written as

$$h_2 = \frac{\sum' x_i (H_{20i} + \int_{T_1}^{T_2} C_{p_i} dT)}{\sum' x_i m_i} \quad (23)$$

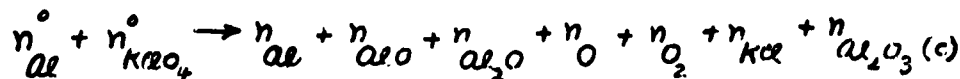
Here  $C_{p_i}$  and  $H_{20i}$  are molar specific heat and enthalpy at  $T_1 = 298.15^\circ\text{K}$  respectively for each product species.

The mixture is 60/40, by weight, of potassium perchlorate/aluminum. The loading density of the powder is 1.5 grams/cm ( $\rho_1 = 1.5$ ). Thus, considering a volume of 1 cm<sup>3</sup>, the combustion involves the following moles ( $n_{\text{Al}}^\circ$  and  $n_{\text{KClO}_4}^\circ$ ) of reactants:

$$\frac{0.4 \rho_1}{m_{\text{Al}}} = \frac{0.4 \times 1.5}{26.98} = n_{\text{Al}}^\circ \quad \frac{0.6 \rho_1}{m_{\text{KClO}_4}} = \frac{0.6 \times 1.5}{138.553} = n_{\text{KClO}_4}^\circ$$



The chemical reaction that will be used is



All products except  $Al_2O_3$  (condensed) are considered to be in the gaseous state in the range of product temperatures of interest. For forming mole fractions from the  $n_i$  it is found convenient to use  $N$  as defined below, omitting the condensed species, as the normalizing factor and make adjustments as required for the condensed  $Al_2O_3$ .

$$N = n_{Al} + n_{Al_2O} + n_{Al_2O} + n_O + n_{O_2} + n_{KCl} \quad (24)$$

$$1 = x_{Al} + x_{Al_2O} + x_{Al_2O} + x_O + x_{O_2} + x_{KCl} \quad (24a)$$

The combustion provides three material balance equations (e.g. aluminum can only go into aluminum-containing species). These are

$$n_{Al} + n_{Al_2O} + 2n_{Al_2O} + 2n_{Al_2O_3} = n_{Al}^{\circ} = 0.0222 \quad (25)$$

$$n_{Al_2O} + n_{Al_2O} + n_O + 2n_{O_2} + 3n_{Al_2O_3} = 4n_{KClO_4}^{\circ} = 0.0260 \quad (26)$$

$$n_{KCl} = n_{KClO_4}^{\circ} = 0.0065 \quad (27)$$

where the right sides are the number of moles per  $cm^3$  provided initially. These can be rewritten in terms of mole fractions.

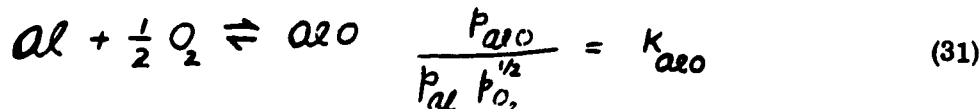
$$x_{Al} + x_{Al_2O} + 2x_{Al_2O} + 2x_{Al_2O_3} = n_{Al}^{\circ}/N \quad (28)$$

$$x_{Al_2O} + x_{Al_2O} + x_O + 2x_{O_2} + 3x_{Al_2O_3} = \frac{4n_{KClO_4}^{\circ}}{N} \quad (29)$$

$$x_{KCl} = \frac{n_{KClO_4}^{\circ}}{N} \quad (30)$$

Since we consider that equilibrium exists among the products, for each molecular species involving Al and  $O_2$  we can write an equilibrium reaction and an equation for the equilibrium constant, which is a tabulated

function of temperature. For example:



Note that the use of  $\text{O}_2$  as the source of oxygen results in fractional powers. However, the available tables give the equilibrium constants for  $\text{O}_2$  as the oxygen source. We can circumvent this difficulty as follows: Consider the reaction written as  $\text{Al} + \text{O} \rightleftharpoons \text{Al}_2\text{O}$  for which

$$\frac{p_{\text{Al}_2\text{O}}}{p_{\text{Al}} p_{\text{O}}} = K'_{\text{Al}_2\text{O}} = \frac{K_{\text{Al}_2\text{O}}}{K_{\text{O}}}$$

since

$$K'_{\text{Al}_2\text{O}} = \frac{p_{\text{Al}_2\text{O}}}{p_{\text{Al}} p_{\text{O}}} \cdot \frac{p_{\text{O}_2}^{1/2}}{p_{\text{O}_2}^{1/2}} = K_{\text{Al}_2\text{O}} \frac{p_{\text{O}_2}^{1/2}}{p_{\text{O}}} = \frac{K_{\text{Al}_2\text{O}}}{K_{\text{O}}}$$

Thus we can use reactions based on O, eliminating fractional powers, except for O, by combining tabulated equilibrium constants in appropriate fashion. Further, we can use the fact that the partial pressures  $p_i = x_i p_2$  to write the equilibria equations in terms of the mole fractions. The vapor pressure of  $\text{Al}_2\text{O}_3(\text{c})$  is considered negligible, and is included in the tabulated equilibrium constant for  $\text{Al}_2\text{O}_3(\text{c})$ . The resulting equations are:

$$\frac{x_{\text{Al}_2\text{O}}}{x_{\text{Al}} x_{\text{O}}} = \frac{K_{\text{Al}_2\text{O}}}{K_{\text{O}}} p_2 = a(T_2) p_2 \quad (32)$$

$$\frac{x_{\text{Al}_2\text{O}}}{x_{\text{Al}}^2 x_{\text{O}}} = \frac{K_{\text{Al}_2\text{O}}}{K_{\text{O}}} p_2^2 = b(T_2) p_2^2 \quad (33)$$

$$\frac{1}{x_{\text{Al}}^2 x_{\text{O}}} = \frac{K_{\text{Al}_2\text{O}_3(\text{c})}}{K_{\text{O}}^3} p_2^5 = c(T_2) p_2^5 \quad (34)$$

$$\frac{x_{\text{O}}}{x_{\text{O}_2}^{1/2}} = K_{\text{O}} p_2^{-1/2} = d(T_2) p_2^{-1/2} \quad (35)$$

The functions a, b, c, and d are defined in the above equations.

Equation 21 combined with 23, equation 24 or 24a, and equations 22,

28, 29, 30, 32, 33, 34, and 35 constitute ten equations in the eleven unknowns

$$p_2 \quad p_2 \quad T_2 \quad N \quad x_{O_2} \quad x_{H_2O} \quad x_{H_2} \quad x_{CO} \quad x_{CO_2} \quad x_{H_2O} \quad x_{O_2}$$

These equations represent simple conservation of mass, momentum, energy, equation of state, material balances, and equilibrium conditions. There is one more unknown than equations and as stated the approach is to use  $T_2$  as a parameter and seek a solution. It was found possible to reduce this system of equations to a single polynomial equation in  $\xi = (p_2 x_{O_2})^{-1/2}$ . Since the reduction procedure with appropriate modifications is applicable to other problems, it is given in detail in Appendix B. For each temperature, the positive real roots of the polynomial which lead to positive pressures were the only physically significant ones. The problem was programmed for the IBM 709 computer and after these roots were found, the downstream values of the unknowns were calculated. The values obtained were unique and are listed in Table 3 as a function of temperature.

#### Numerical Results and Discussion

The values in Table 3 were selected from the full computation, which was done for temperatures 100°K apart. As expected, one finds a deflagration branch, a physically impossible dead zone (contradicts conservation of mass and momentum), and a detonation branch. The detonation results must be regarded as of limited validity because of the assumptions d, e, f, and g made at the beginning of this section. Three conclusions follow immediately.

a. Deflagration can occur only, for temperatures at the rear of the stable reaction zone, below 4000°K and only with flame speeds of the order of cm/sec.

b. The dead zone extends from 4000°K upwards to a temperature approaching 7000°K, the exact value depending on the limiting assumptions d, e, f, and g.

c. A Chapman-Jouguet detonation can be expected to have a temperature in the neighborhood of 7000°K.

The OPHCT has served to confirm once again that the experimentally

observed phenomena are not those of a deflagration. There are other extensions of OPHCT (covolumes, other product species, incomplete combustion of Al) which could be carried out but they would not change this conclusion. For this reason, we turn now to calculating the Chapman-Jouguet detonation for the mixture.

## CHAPMAN-JOUGUET DETONATION CONSIDERATIONS

The calculation of the speed of an ideal detonation differs from that of a deflagration in that the system of equations is complete. This is achieved by the addition of the Chapman-Jouguet stability condition. The problems with respect to the detonation calculation stem from the high pressures (e.g. 100,000 atmospheres) in the detonation zone. The equation of state of the gaseous products, that for solid products, and the choice of products and of thermodynamic data must all be appropriate to the anticipated higher pressures. The Chapman-Jouguet values are calculated by computer. At Los Alamos Scientific Laboratories a Brinkley-Kistiakowsky-Wilson (BKW) technique is used. At Lawrence Radiation Laboratory a similar program which can handle two condensed product species is used. The latter, called RUBY (Ref 33) was made available to Picatinny Arsenal where it was used for the calculations described in this report. The RUBY program uses a Kistiakowsky-Wilson equation of state for the product gases (Refs 34, 47). It requires one to choose the products, provide thermodynamic data for them and equations of state for the condensed products. The choices made and parametric studies of the significance of these decisions are given below. This is followed by a presentation and discussion of the results.

### Inputs and Parametric Studies

The products chosen differ from those of OPHCT in two important regards. The gaseous product  $\text{Al}_2\text{O}_3$  is considered to exist at the high pressures. It is recognized that the literature (Refs 35-39) indicates that  $\text{Al}_2\text{O}_3$  gas decomposes, producing suboxides. However, although this is true at very low pressures compared to those of a detonation, experience with calculations on explosives containing aluminum indicates a need for  $\text{Al}_2\text{O}_3$  gas to obtain correct results. The other difference from OPHCT is that the KCl is permitted to decompose completely and react, thus allowing for the additional species K,  $\text{K}_2$ , and  $\text{AlCl}_3$ . The

suboxides of aluminum have again been included. The condensed species expected are Al (s) and Al<sub>2</sub>O<sub>3</sub> (s). The species used are listed in Table 5.

Thermodynamic tables for the products are available from many sources (Refs 40-46). Here, too, one must be careful to select data appropriate for high pressures. The RUBY program minimizes the free energy to find the chemical equilibrium among the products for the T and p under consideration. The free energy is computed from specific heat vs temperature tables. If such tables have simply assumed a constant specific heat for high temperatures, this will affect the computation. Unfortunately, this occurs occasionally in the JANAF tables (Ref 43) and for such species the JANAF tables were not used. The JANAF data were used in the form of the generating polynomials (Ref 44). However, most of the thermodynamic data were taken from the LASL compilation (Ref 45), which has a history of successful use in detonation calculations. The thermodynamic data used in the calculation are listed in Table 5.

The covolumes for the gaseous species are (Refs 34, 47) equal to 10.46 V<sub>i</sub>, where V<sub>i</sub> is the molecular volume in Å<sup>3</sup>. For KCl the molecular volume was calculated, assuming full rotatibility, using (Ref 48) an equilibrium internuclear distance of 2.671 Å, and Van derWaal radii for Cl and K of 1.80 Å and 2.825 Å, respectively. The last value was calculated by assuming that the Van derWaal radii can be taken as equal to covalent radius plus 0.80 Å. The covolumes used are shown in Table 5.

The equations of state at high pressures for Al (s) and Al<sub>2</sub>O<sub>3</sub> (s) were of the form used by Cowan and Fickett (Ref 34).

$$\begin{aligned}
 p &= p_i(V_i) + a(V_i) T + b(V_i) T^2 \\
 &= A_0 + A_1 Y + A_2 Y^2 + A_3 Y^3 + A_4 Y^4 \\
 &\quad + (B_0 - B_1 Y) T + \left( C_0 + \frac{C_1}{Y} + \frac{C_2}{Y^2} \right) T^2
 \end{aligned}$$

Here Y = initial specific volume/ specific volume at T and p. The A<sub>i</sub> coefficients used were those of the shock Hugoniot for Al (s) (Ref 49) and Al<sub>2</sub>O<sub>3</sub> (s) (Ref 50) used as an adequate approximation to this part of the equation of state. The coefficients B<sub>0</sub> and B<sub>1</sub> were determined using thermal expansion (Ref 51) and compressibility data (Ref 52). (The

former data were also used for generating a thermal expansion equation which is also required.) The coefficients  $C_0$ ,  $C_1$ , and  $C_2$  are associated with electronic vibrations and (for the pressures obtained with this mixture) can be set equal to zero. The coefficients for the equations of state and thermal expansion equation are listed in Table 5.

The principal calculation made use of the best data available. However, other runs were made to determine how the results depended on the data used. The equations of state were deleted and the solids treated as incompressible. In a second variation, some of the thermodynamic data from LASL were replaced by JANAF data. The effect of loading density of the mixture was evaluated by changing the value from 1.5 to 0.5 g/cm<sup>3</sup>. Dr. C. Mader of LASL was kind enough to calculate the C-J values with his BKW code. Since several less important species were omitted by him, this provided both a measure of their effect and by virtue of the agreement with the principal RUBY calculation a corroboration thereof.

#### Numerical Results

The results of the RUBY calculations of the Chapman-Jouguet detonation for the mixture are shown in Table 6. Although a variety of input conditions are represented, the results all show that the calculated detonation velocity is several times the highest experimentally observed value.

From the results one can also conclude the following: The equations of state should be included in any calculation. Both Al (s) and Al<sub>2</sub>O<sub>3</sub> (s) are required. Although some gaseous species (e.g., Al<sub>2</sub>O<sub>2</sub>) could be omitted for this mixture and others such as Al<sub>2</sub>O<sub>3</sub> (g), AlCl<sub>3</sub> (g) should not be omitted, it would be best for a similar mixture to include all those listed. The thermodynamic data, as expected, affect the results. A reduction in density reduces the detonation velocity and pressure and Al<sub>2</sub>O<sub>3</sub> (s) is no longer present.

## OVERALL DISCUSSION

The sections on diffusivity and sound speed considerations and the OPHCT theory established that the propagation of combustion was not deflagrative. The calculated Chapman-Jouguet detonation velocity was about 3 to 4 times the highest experimentally observed speed of the flame front. However, this last result only indicates that we are not dealing with an ideal detonation.

In the ideal detonation, the problem is considered as strictly one dimensional with a reaction zone of negligible thickness. The experimental results showed a reaction zone several centimeters long and considerable lateral rarefaction starting within one centimeter of the front. Hence one possible explanation of the discrepancy between the RUBY and experimental results is the lateral rarefaction.

The RUBY calculation is not designed for calculations that include relaxation phenomena associated with physical kinetics of the mixture. In the mixture, there are aluminum particles that require times to vaporize that are significant fractions of the time required by the reaction zone to pass a fixed point. In the experimental results, this slower release of the fuel would affect the flame speed. This is in accord with the previously reported (Ref 4) dependence of combustion on particle size, and the observed structure of the reaction zone. The presence of two reaction zone profiles with different speed ranges also indicates the presence of some rate phenomena. Similar physical effects have been reported for nitrocellulose or nitroglycerin powder (Ref 53), liquid nitroglycerin or methyl nitrate (Refs 54, 55), flaked TNT and composition B (Refs 56, 57, 58), and others (Ref 59). Hence another possible explanation of the divergence of the RUBY results from the observations is that one must include physical kinetics in the calculation.

### Further Experimental Work

The effect of lateral rarefaction could be evaluated by altering the confinement of the column of mixture and using larger diameter columns. Other worthwhile modifications include using longer propagation sticks, varying the mode of initiation, and examining the reaction zone by time-resolved spectroscopy. In addition, it would be worthwhile reviewing the experimental work on low speed detonations to observe the techniques used by others.

### **Further Theoretical Work**

Using the experimental data to give a measure of the lateral rarefaction rate and ignoring the relaxation effects of the medium, one can calculate estimates of the lateral effect on the detonation velocity. This could then be compared with the experimental results.

The area in which it is believed there is a greater contribution to be made is that of the relaxation effects. Prior to working on this problem, it would be necessary to review in detail studies of reaction zone structure (Refs 60-64) with a view to substituting or adding physical kinetic considerations (vaporization, diffusion) to the chemical reaction rates considered. Another approach would be based on a two-phase flow theory (Ref 65) where the solution would depend on the assumptions made on mass and energy interchange and forces acting between the two phases. Finally, one can explore the concepts used for detonations in dilute sprays (Ref 66). An explanation of low speed detonations and the experimental observations on this mixture would be the objectives of the theoretical work.



## ACKNOWLEDGEMENTS

It is a pleasure to acknowledge the many stimulating discussions with Dr. B. T. Chu of Brown University and his participation in several calculations.

The author wishes to thank Mr. I. Klugler of this Laboratory who provided all the necessary programming analysis.

The RUBY code used herein was written at the Lawrence Radiation Laboratory (Livermore).

Dr. Charles L. Mader of the Los Alamos Scientific Laboratory discussed the calculation of the Chapman-Jouguet values by the BKW technique with the author and made several helpful suggestions.

Mr. N. Coburn of NOL was kind enough to furnish some preliminary results of measurements of the shock Hugoniot of solid aluminum oxide.

The work was supported initially by the Pyrotechnics Laboratory, FRL, as part of its program of Basic and Technical Research, and completed under sponsorship of the Terminal Ballistics Laboratory, BRL.

## REFERENCES

1. Hershkowitz, J., "The Action of an Explosive on Surrounding Non-reacting Metal Dust," Picatinny Arsenal Technical Report 2484, December 1957
2. Hershkowitz, J., "The Mechanism of Ignition and Propagation of Oxidant-Metal Flashes," Picatinny Arsenal Technical Report 2526, April 1958
3. Hershkowitz, J. and Schwartz, F. R., "Propagation of Chemical Reaction Zones in an Oxidant-Metal Dust Mixture," Bull. Am. Phys. Soc. II, 4, No. 3, p 205 (30 March 1959)
4. Hershkowitz, J., Schwartz, F., and Kaufman, J. V. R., "Combustion in Loose Granular Mixtures of Potassium Perchlorate and Aluminum," Eighth Symposium (International) on Combustion, The Williams & Wilkins Company, Baltimore 2, Md (1962) Paper No. 76, pp 720-727
5. Courant, R., and Friedrichs, K. O., Supersonic Flow and Shock Waves, pp 204-235, Interscience Publishers, Inc., New York (1956)
6. Evans, M. W., and Ablow, C. M., "Theories of Detonation," Chemical Reviews, 61 pp 129-178 (April 1961)
7. Carslaw H. S., and Jaeger J. C., Conduction of Heat in Solids, p 9, Oxford University Press, Second Edition (1959)
8. Handbook of Chemistry and Physics, Chemical Rubber Publishing Co. (Annual)
9. Bird, R. B., Stewart, W. E., and Lightfoot, E. N., Notes on Transport Phenomena, pp 302-308, Wiley (1958)
10. Hirschfelder, J. O., Curtiss, C. F., and Bird, R. B., Molecular Theory of Gases and Liquids, pp 720-724, Wiley (1954)
11. Chu, B. T., "Thermodynamics of a Dusty Gas and its Application to Some Aspects of Wave Propagation in the Gas," p 12, Brown University Report DA-4761/1 (June 1960), Contract No. DA-19-020-ORD-4761
12. Chu, B. T., "Thermodynamics of Porous Elastic Solid Containing a Compressible Fluid," Brown University Report DA-4761/2 (June 1960) Contract No. DA-19-020-ORD-4761

13. Love, A. , A Treatise on the Mathematical Theory of Elasticity, p 108, 4th Ed., Dover (1927)
14. Landau, L. D. , and Lifshitz, E. M. , Theory of Elasticity, p 11, Addison Wesley (1959)
15. Reiner, M. , Lectures on Theoretical Rheology, p 40, Interscience (1960)
16. Kolsky, H. , Stress Waves in Solids, p 201, Oxford (1953)
17. Chu, B. T. , "Thermodynamics of a Loosely Packed Granular Aggregate," Brown University Report DA-4761/3 (June 1962), Contract No. DA-19-020-ORD-4761
18. Sakurai, T. , "Propagation Velocities of Shock Waves in Air and in Powders by Explosives," Journal of the Industrial Explosives Society of Japan, 16(2): 90-94, 1955 (in Japanese)
19. Exner, M. L. , "Investigation of the Acoustical Behaviour of Powders under Excitation of Shear Waves," Acustica 4, pp 350-358 (No. 2, 1954) (in German)
20. Daniel, A. , " Stress-Strain Characteristics of a Granular Material," Engineering 184, 4766 pp 45-46
21. Gassman, F. , "The Elasticity of Porous Media," Mitt. Inst Geophysics, E. T. H. Zurich, No. 17, 23 pp (1951) (in German) (summary in Physics Abstracts 54, 9743 (1951))
22. Duffy, J., and Mindlin, R. D. , "Stress-Strain Relations and Vibrations of a Granular Medium," J. Appl. Mech. 24, 4, pp. 585-93 (Dec 1957)
23. Gassman, F. , "Elastic Waves Through a Packing of Spheres," Geophysics 16, 673-85, (October 1951)
24. Morse, R. W. , "Acoustic Propagation in Granular Media," J. Acoust. Soc. Am. 24, 696 (Nov 1952)
25. Thomas, L. H. , "An Approach to the Theory of Shock Waves in Air Sand Mixtures," BRL Memorandum Report 871, Feb 1955
26. Carrier, G. F. , "The Transmission of Blast Through a Dust Filled Gas," BRL Memorandum Reports 872 and 873, Feb 1955

27. Chambre, P. L., "Speed of a Plane Wave in a Gross Mixture," J. Acoust. Soc. Am. 26, 329 (May 1954)
28. Katz, S., and Alvrens, T. J., "Properties of Plane Waves in Granular Materials," Rensselaer Polytechnic Research Division, Troy, N. Y. Tech Reports 1, 2 on BRL Contr. No. DA-30-115-509-ORD-1009 (Dec 1959 and Sept 1960)
29. Markstein, G. A., and Polanyi, M., "Flame Propagation, A Critical Review of Existing Theories," Cornell Aeronautical Laboratories Bumblebee Series Report No. 61 (April 1947)
30. Penner, S.S., and Jacobs, T. A., "Combustion and Flames," California Institute of Technology Technical Report No. 29 on Contract DA-04-495-ORD-1634 (Nov 1959)
31. Copp, J. L., and Ubbelohde, A. R., "Physico-Chemical Processes Occurring at High Pressures and Temperatures. Pt II - The Effect of Inert Components on Detonation." Trans. Faraday Soc. 44 Pt. 9 pp 658-669 (Sept 1948)
32. Jones, M. M., Ling, R. C., Alster J., and Flanagan, T. B., "Survey of Equations of State for Use with Dense Primary Explosives," Picatinny Arsenal Technical Report 2483 (June 1958)
33. Levine, H. B., and Sharples, R. E., "Operators Manual for RUBY," Lawrence Radiation Laboratory, University of California, Livermore, California. (Rough Draft Feb. 13, 1962)
34. Cowan, R. D., and Fickett, W., "Calculation of the Detonation Properties of Solid Explosives with the Kistiakowsky-Wilson Equation of State," J. Chem. Phys., 24, 932 (1956)
35. Brewer, L., and Searcy, A. W., "The Gaseous Species of the Al-Al<sub>2</sub>O<sub>3</sub> System," J. Am. Chem. Soc. 76, pp. 5308-5314 (1951)
36. Hoch, M., and Johnston, H. L., "Formation, Stability and Crystal Structure of the Solid Aluminum Oxides, Al<sub>2</sub>O and AlO," J. Am. Chem. Soc. 76, pp. 2560-2561 (1954)
37. Porter, R. F., Schisel, P., and Inghram, M. G., "A Mass Spectroscopic Study of Gaseous Species in Al-Al<sub>2</sub>O<sub>3</sub> System," J. Chem. Phys. 23 pp. 339-342 (1955)

38. Farber, M., "Thermodynamics of  $\text{Al}_2\text{O}_3$ ," Jet Propulsion, 28 pp. 760-761 (1958)
39. Cook, M. A., Filler, A. S., Keyes, R. T., Partridge, W. S., and Ursenback, W. O., "Aluminized Explosives," J. Phys. Chem. 61, pp. 189-196 (1957)
40. Rossini, F. D., Wagman, D. D., Evans, W. H., Levine, S., and Jaffe, T., "Selected Values of Chemical Thermodynamic Properties," National Bureau of Standards Circular 500 and Supplement (Feb and April 1952)
41. Douglas, T. B., "Preliminary Report on the Thermodynamic Properties of Selected Light Element Compounds," National Bureau of Standards Fourth Technical Summary Report No. 6298 (July 1960). This supplements No. 6297 (Jan. 1959), No. 6484 (July 1959) and No. 6645 (Jan. 1960)
42. Gordon, J. S., "Thermodynamic Data for Combustion Products," Reaction Motors Report RMD 210-E3 (Jan. 1960) (Contract AF33(616) - 5639)
43. Dergazarian, T. E., and others, JANAF Interim Thermochemical Tables, Dow Chemical Co. on Contract No. AF33(616) - 6149. Vol. 1, 2 (Dec 1960) Revision and Supplements May, Dec. 1961, May-June 1962
44. Wiederkehr, R. R. V., "A General Method for Calculating the Specific Impulse of Propellant Systems," Report Nrs. AR-1S-60 and AR-3S-61, Computations Research Laboratory, Dow Chemical Company, (1960-1)
45. Mader, C. L., "Thermodynamic Properties of Detonation Products," Los Alamos Scientific Laboratory, University of California, Report GMX-2-R-59-3 (Sept. 1959) and Supplement, Report GMX-2-R-60-1 (April 1960)
46. Brewer, L., "The Thermodynamic Properties of the Alkali Halides," University of California, UCRL 9952 (Nov 1961)
47. Mader, C. L. "Detonation Performance Calculations Using the Kistiakowsky-Wilson Equation of State, " Los Alamos Scientific Laboratory, LA 2613 (Oct 1961)
48. Pauling, L., The Nature of the Chemical Bond, Third Edition (1960), Cornell University Press pp 79, 257, 260, 263, 532

49. Rice, M. H., McQueen, R. G., and Walsh, J. M., "Compression of Solids by Strong Shock Waves," p 32, Vol 6 of Solid State Physics, edited by F. Seitz and D. Turnbull, Academic Press (1958)
50. Coburn, N., Naval Ordnance Laboratory, Silver Springs, Md., Informal Communication of Preliminary Data
51. Goldsmith, A., Waterman, T. E., and Hirschhorn, H. J., Handbook of Thermophysical Properties of Solid Materials, Table VII-A-1-a for  $\text{Al}_2\text{O}_3$  and I-A-2 for Al. The Macmillan Co., N.Y. (1961)
52. Wachtman, J. B. Jr., and Lam, D. G., "Young's Modulus of Refractory Materials as Function of Temperature," J. Am. Ceramic Soc. 42, p 258 (May 1959)
53. Urbanski, T., Z. f. ges. Schiess - Sprengstoffe, 34, 103 (1939)
54. Ratner, S. B., and Chariton, J. B., Doklady Ak. Nauk SSSR. 40, 293 (1943)
55. Ratner, S. B., Doklady Ak. Nauk SSSR, 42, 276, (1944)
56. Jones, E., and Mitchell, D., Nature 161, 98 (1948)
57. Cook, M., "Some Framing Camera Studies of Phenomena Associated with the Detonation of High Explosives," University of Utah Explosives Research Group Tech. Rept II on Contract No. N7-onr-45107 Proj. N 357239 (7 May 1956)
58. Malin, M. E., Campbell, A. W., and Moutz, C. W., "Particle Size Effects in Explosives at Finite and Infinite Diameters," J. Appl. Phys. 28, pp 63-69 (Jan 57)
59. Deffet, L., and Boucart, J., "A Study of Detonation Waves by X-Ray Flashes," Discussions Faraday Soc. 22, pp 167-71 (1956)
60. Hirschfelder, J. O., and Curtiss, C. F., J. Chem. Phys. 28 1130 (1958)
61. Linder, B., Curtiss, C. F., and Hirschfelder, J. O., J. Chem. Phys. 28 1147 (1958)
62. Curtiss, C. F., Hirschfelder, J. O., Barnett, M. P., J. Chem. Phys. 30, 470 (1959)
63. Wood, W. W., Phys. Fluids, 4, 46 (1961)

64. Talbot, L., ARS Journal, 32, 1009 (1962)
65. Chu, B. T., and Parlange, J. Y., "A Macroscopic Theory of Two Phase Flow with Mass, Momentum and Energy Interchange," Brown University Report DA-4761/4 (June 1962) Contract DA-19-020-ORD-4761
66. Williams, F. A., "Detonations in Dilute Sprays," p 99 in Detonation and Two-Phase Flow, edited by S. S. Penner and F. A. Williams, Academic Press (1962)

Table 1  
Data on the Compression of Aluminum Powder\*\*\*

$\frac{V_0 - V^{**}}{V_0}$	$F_0^*$	$\frac{V_0 - V^{**}}{V_0}$	$F_0^*$
0.	0.	0.1178	75.01
0.0036	0.01379	0.1206	78.60
0.0078	0.09652	0.1228	82.18
0.0120	0.2620	0.1261	85.21
0.0162	0.5515	0.1283	89.19
0.0196	0.9928	0.1293	92.93
0.0230	1.599	0.1331	96.80
0.0271	2.303	0.1363	100.10
0.0298	3.185	0.1395	104.78
0.0332	4.247	0.1422	107.83
0.0398	6.673	0.1469	115.83
0.0424	8.053	0.1495	121.07
0.0463	9.652	0.1520	124.1
0.0528	12.961	0.1556	129.06
0.0541	14.89	0.1581	132.37
0.0579	16.82	0.1602	137.34
0.0610	18.75	0.1632	140.65
0.0635	20.96	0.1657	144.51
0.0673	23.33	0.1682	148.92
0.0691	24.93	0.1706	153.88
0.0759	30.23	0.1736	157.19
0.0789	32.96	0.1755	162.43
0.0820	35.58	0.1789	165.47
0.0850	37.89	0.1808	170.98
0.0879	40.54	0.1832	175.12
0.0903	43.30	0.1859	179.25
0.0933	46.05	0.1880	184.77
0.0962	49.09	0.1905	189.18
0.0997	52.12	0.1929	193.04
0.1049	58.18	0.1950	198.56
0.1077	61.50	0.1975	203.52
0.1100	65.08	0.1999	207.38
0.1128	68.11	0.2024	212.35
0.1150	71.49	0.2045	217.86



Table 1 (Continued)

Data on the Compression of Aluminum Powder\*\*\*

$\frac{V_0 - V^{**}}{V_0}$	$F_0^*$	$\frac{V_0 - V^{**}}{V_0}$	$F_0^*$
222.00	0.2074	0.2205	252.34
226.14	0.2094	0.2234	256.47
231.65	0.2119	0.2251	261.99
237.17	0.2135	0.2271	267.50
242.68	0.2156	0.2300	271.64
247.65	0.2181		

\* Values of  $F_0$  (pressure) shown, after multiplication by  $10^6$ , are in c.g.s. units.

\*\* A reference of  $V_0 = 1/\rho = \frac{1}{1.4}$  has been used as the starting point for significant pressures. The actual pressure was 0.0120 dynes/cm<sup>2</sup>.

\*\*\* Least square fits using polynomials up to and including the 7th degree were tried for the entire data and with the data divided in two parts. The results chosen as most suitable for sound speed calculations were

$$\text{for } X \equiv \frac{V_0 - V}{V_0} \leq 0.05786 \quad F_0 = A_0 + A_1X + A_2X^2 + A_3X^3 + A_4X^4 + A_5X^5$$

$$\text{with } A_0 = -0.871223 \times 10^{-2}$$

$$A_1 = -0.311934 \times 10^4$$

$$A_2 = 0.194468 \times 10^2$$

$$A_3 = 0.330135 \times 10^6$$

$$A_4 = -0.524995 \times 10^7$$

$$A_5 = 0.325772 \times 10^8$$

$$\text{for } X \equiv \frac{V_0 - V}{V_0} > 0.05786 \quad F_0 = A_0 + A_1X + A_2X^2 + A_3X^3 + A_4X^4$$

$$\text{with } A_0 = 0.234946 \times 10^2$$

$$A_1 = -0.942820 \times 10^3$$

$$A_2 = 0.178666 \times 10^5$$

$$A_3 = -0.658572 \times 10^5$$

$$A_4 = 0.115540 \times 10^6$$

Table 2  
Sound Speed Results for the Granular Aggregate Model

Density (g/cm <sup>3</sup> )	Speed (m/sec)
1.40	37.1
1.45	151
1.50	206
1.55	250
1.60	269
1.65	280
1.70	289
1.75	299
1.80	312
1.85	328
1.90	346
1.95	365
2.00	386
2.05	407
2.10	427
2.15	447
2.20	466
2.25	484
2.30	499
2.35	513

Table 3

One-Parameter Hydrodynamic Combustion Theory Results

T° K	U (cm/s)	v <sub>2</sub> (cm/s)	ρ <sub>2</sub> (gm/cm <sup>2</sup> )	p <sub>2</sub> (bars)*	
<u>Deflagration Branch</u>					
3000	2.26	2.92 x 10 <sup>5</sup>	1.16 x 10 <sup>-5</sup>	0.02	
3500	3.70	1.57 x 10 <sup>5</sup>	3.53 x 10 <sup>-5</sup>	0.14	
3900	0.61	4.94 x 10 <sup>3</sup>	1.84 x 10 <sup>-4</sup>	1.00	
<u>Dead Zone</u> (p <sub>2</sub> > p <sub>1</sub> but ρ <sub>2</sub> < ρ <sub>1</sub> (1.5))					
4000	8.48	4.57 x 10 <sup>4</sup>	2.79 x 10 <sup>-4</sup>	1.57	
7000	2.45 x 10 <sup>5</sup>	2.68 x 10 <sup>5</sup>	1.38	8.09 x 10 <sup>3</sup>	
<u>Detonation Branch</u>					
7100	3.8 x 10 <sup>5</sup>	3.63 x 10 <sup>5</sup>	1.57	9.52 x 10 <sup>3</sup>	
7600	1.76 x 10 <sup>5</sup>	1.05 x 10 <sup>5</sup>	2.51	1.86 x 10 <sup>4</sup>	
T° K	X <sub>O</sub>	X <sub>Al</sub>	X <sub>AlO</sub>	X <sub>Al<sub>2</sub>O</sub>	X <sub>O<sub>2</sub></sub>
3000	2.0 x 10 <sup>-2</sup>	1.8 x 10 <sup>-1</sup>	3.2 x 10 <sup>-2</sup>	1.9 x 10 <sup>-1</sup>	6.8 x 10 <sup>-4</sup>
3500	2.2 x 10 <sup>-1</sup>	1.6 x 10 <sup>-1</sup>	1.1 x 10 <sup>-1</sup>	1.6 x 10 <sup>-1</sup>	2.9 x 10 <sup>-2</sup>
3900	2.5 x 10 <sup>-1</sup>	1.5 x 10 <sup>-1</sup>	1.3 x 10 <sup>-1</sup>	1.7 x 10 <sup>-1</sup>	4.4 x 10 <sup>-2</sup>
7100	5.8 x 10 <sup>-2</sup>	7.1 x 10 <sup>-2</sup>	1.2 x 10 <sup>-1</sup>	2.3 x 10 <sup>-1</sup>	8.4 x 10 <sup>-4</sup>
7600	3.7 x 10 <sup>-2</sup>	1.0 x 10 <sup>-1</sup>	1.5 x 10 <sup>-1</sup>	1.9 x 10 <sup>-1</sup>	1.7 x 10 <sup>-6</sup>
		X <sub>KCl</sub>		X <sub>Al<sub>2</sub>O<sub>3</sub>(c)</sub>	
		5.8 x 10 <sup>-1</sup>		6.9 x 10 <sup>-1</sup>	
		3.1 x 10 <sup>-1</sup>		2.3 x 10 <sup>-1</sup>	
		2.5 x 10 <sup>-1</sup>		1.3 x 10 <sup>-1</sup>	
		5.1 x 10 <sup>-1</sup>		5.5 x 10 <sup>-1</sup>	
		5.2 x 10 <sup>-1</sup>		5.6 x 10 <sup>-1</sup>	

\* 1 atmosphere = 1.01325 bars =  $1.01325 \times 10^6$  dynes/cm<sup>2</sup>

Table 4  
Tentative Hugoniot Data for  $\text{Al}_2\text{O}_3$  (s) \*

<u><math>p</math> (megabars)</u>	<u><math>Y^{**}</math></u>
0	1
0.02655	1.0141
0.05528	1.0275
0.08619	1.0401
0.11927	1.0522
0.15453	1.0637
0.19193	1.0746
0.23157	1.0850
0.27339	1.0948
0.31761	1.1042

$$A_0 = 0.800285\text{E}-5 \quad A_1 = -0.428736\text{E}2 \quad A_2 = 0.131033\text{E}3$$

$$A_3 = -0.13509\text{E}3 \quad A_4 = 0.469329\text{E}2$$

in  $p = A_0 + A_1 Y + A_2 Y^2 + A_3 Y^3 + A_4 Y^4$

by least squares fit

---

\* These preliminary data were supplied in different form as a courtesy by N. Coburn, Naval Ordnance Laboratory, Silver Springs, Md.

\*\*  $Y = 0.27027 /$  specific volume at  $p$  of shock.

Table 5  
RUBY Input Data

Thermodynamic Data

Species	Specific Heat Source	Covolume*	Heat of Formation**	Free Energy of Formation**
Al	LASL	350	3.2659	2.8597
AlO	DOW	1160	0.8959	0.6350
Al <sub>2</sub> O	DOW	1300	-1.3164	-1.6121
Al <sub>2</sub> O <sub>2</sub>	DOW	1800	-3.9943	-4.0258
Al <sub>2</sub> O <sub>3</sub>	LASL	1350	-10.0769	-9.8861
AlCl <sub>3</sub>	LASL	2600	-5.8795	-5.7366
K	LASL	920	0.8998	0.6123
K <sub>2</sub>	LASL	4600	1.2869	0.9222
K Cl	LASL	2800	-2.1605	-2.3530
O <sub>2</sub>	DOW	350	0.0	0.0
O	DOW	120	2.4937	2.3194
Al <sub>2</sub> O <sub>3</sub> (s)	LASL	24.485	-16.7647	-15.8301
Al(s)	LASL	9.9889	0.0	0.0

---

\* In cm<sup>3</sup>/mole. For solids, value is volume in cm<sup>3</sup> occupied by one mole at initial  $T$  and  $p$ .

\*\* In megabar cm<sup>3</sup> per mole.

Table 5 (Continued)

## Thermodynamic Data (Continued)

Species	GAM 0*	GAM 1	GAM 2	GAM 3	GAM 5
A1	2.4135997	-8.7089276E-3	7.1777077E-3	0.	0.
A1O	4.2483855	1.1573301	-1.8338290	1.5959543	-7.0816294E-4
A1 <sub>2</sub> O	6.5471740	1.5580869	-4.1013633	3.5731770	-1.5859616E-3
A1 <sub>2</sub> O <sub>2</sub>	9.2748740	2.8285952	-7.4501969	6.4935588	-3.2106461E-3
A1 <sub>2</sub> O <sub>3</sub>	12.324936	0.71581680	-0.6036318	0.	0.
A1Cl <sub>3</sub>	9.5651999	0.2642911	-0.2215514	0.	0.
K	2.072784	2.0914092	-1.4225951	0.	0.
K <sub>2</sub>	3.4132741	8.4193720	-3.942406	0.	0.
KCl	4.3330734	0.6990020	-1.9300586E-3	0.	0.
O <sub>2</sub>	3.8926835	3.0720323	0.50698165	-4.6228122	-7.805438E-4
O	2.4786804	-0.91630437	3.4551387	-2.485581	3.7995423E-5
A1 <sub>2</sub> O <sub>3</sub> (s)	13.77977	3.965481	-7.377259	4.357859	0.
A1(s)	2.8406157	0.32750082	-0.4891151	0.	0.

\* The specific heat is in megabar cm<sup>3</sup>/e.v. mole and is given by the following expansion with  $T$  in electron volts.

$$= \text{GAM } 0 + \text{GAM } 1 T + \text{GAM } 2 T^2 + \text{GAM } 3 T^3 + \text{GAM } 4 T^{-1} + \text{GAM } 5 T^{-2} + \text{GAM } 6 T^{-3}$$

The GAMOS coefficients have corresponding units. All GAM 4 and GAM 6 were zero for the data used. (E2 means  $\times 10^2$ , etc.)

Table 5 (Continued)

Equation of State Data\*

	A <sub>0</sub>	A <sub>1</sub>	A <sub>2</sub>	A <sub>3</sub>	A <sub>4</sub>
Al <sub>2</sub> O <sub>3</sub> (s)	-0.800285E-5	-0.428736E2	0.131033E3	-0.13509E3	0.469329E2
Al(s)	0.466	-0.1269E1	0.375	0.428	
	B <sub>0</sub>	B <sub>1</sub>	ALPS	BETS	GAMS
Al <sub>2</sub> O <sub>3</sub> (s)	0.1405	0.22687	1.0092533	-0.36321	0.12721
Al(s)	-0.16284	0.39467	1.0261949	-1.04433	0.98718

\* The pressure is in megabars and is given as a function of  $Y$  = initial volume/volume at  $T$  and  $p$ .

$$p = A_0 + A_1 Y + A_2 Y^2 + A_3 Y^3 + A_4 Y^4 + B_0 + B_1 Y$$

The thermal equation of state relates  $Y$  to  $T$  at atmosphere pressure by

$$Y = ALPS + BETS \cdot T + GAMS \cdot T^2$$

Table 6

Results of RUBY Runs\*\*

Run No.	55	56	47	48	LASL	45
Eq. St. $\text{Al}_2\text{O}_3(\text{s})$	*	INCOMP	INCOMP	INCOMP	INCOMP	INCOMP
Eq. St. $\text{Al}(\text{s})$	*	*	*	*	--	INCOMP
Thermo data	*	*	*	DOW	*	DOW
Species	*	*	*	*	REDUCED	REDUCED
Density	*	*	0.5	*	*	*
<hr/>						
$T^\circ \text{K}$	6267	8731	5775	7372	7290	7372
$p$ megabars	0.1070	0.0944	0.0167	0.0761	0.1026	0.0407
$U$ m/s	4966	4977	3115	4545	4845	3286
$\text{Al}$	3.9E-5	1.2E-4	7.0E-4	3.5E-7	1.9E-3	3.2E-6
$\text{AlO}$	2.1E-7	2.8E-6	1.7E-5	1.2E-7	--	3.2E-6
$\text{Al}_2\text{O}$	7.4E-5	5.7E-5	9.7E-4	7.5E-8	--	7.4E-7
$\text{Al}_2\text{O}_2$	1.1E-7	2.1E-7	2.1E-6	3.6E-9	--	9.1E-8
$\text{Al}_2\text{O}_3$	4.0E-3	4.4E-4	5.4E-3	1.6E-4	1.7E-3	--
$\text{AlCl}_3$	1.3E-3	8.3E-4	4.1E-4	5.2E-5	1.3E-3	--
$\text{K}$	3.8E-3	2.4E-3	1.2E-3	1.5E-4	4.2E-3	--
$\text{K}_2$	9.9E-7	6.1E-5	2.1E-5	2.1E-6	1.8E-6	--
$\text{KCl}$	5.6E-4	1.9E-3	3.1E-3	4.2E-3	1.7E-4	4.3E-3
$\text{O}_2$	2.1E-9	7.1E-8	2.3E-8	1.0E-6	--	1.2E-4
$\text{O}$	6.4E-8	1.8E-6	1.3E-6	2.0E-6	--	9.8E-5
$\text{Al}_2\text{O}_3(\text{s})$	1.7E-3	5.3E-3	0.	5.6E-3	4.1E-3	5.7E-3
$\text{Al}(\text{s})$	1.9E-3	2.3E-3	8.8E-4	3.2E-3	--	3.5E-3

\* Indicates that standard conditions as described in report and Table 5 were used. INCOMP indicates that equation of state was deleted and the solid considered incompressible. A run with density  $0.5 \text{ g/cm}^3$  instead of the usual 1.5 was made. DOW indicates that the thermodynamic data from LASL for  $\text{Al}$ ,  $\text{AlCl}_3$ ,  $\text{Al}_2\text{O}_3(\text{s})$ ,  $\text{Al}(\text{s})$  was replaced by that of DOW. REDUCED indicates that the species indicated by -- in the data column were deleted.

\*\* $U$  is the detonation velocity,  $p, T$  are the Chapman-Jouguet pressure and temperature. Specie concentrations are per gram of initial mixture.



Table 6 (Continued)

The run numbers are local designations and are convenient for reference and making comparisons. LASL is the run made at Los Alamos Scientific Laboratory with the BKW code by Dr. C. Mader. There are a few other differences between runs which are not indicated in the tabulation because the effect on the results was shown separately to be of no significance.

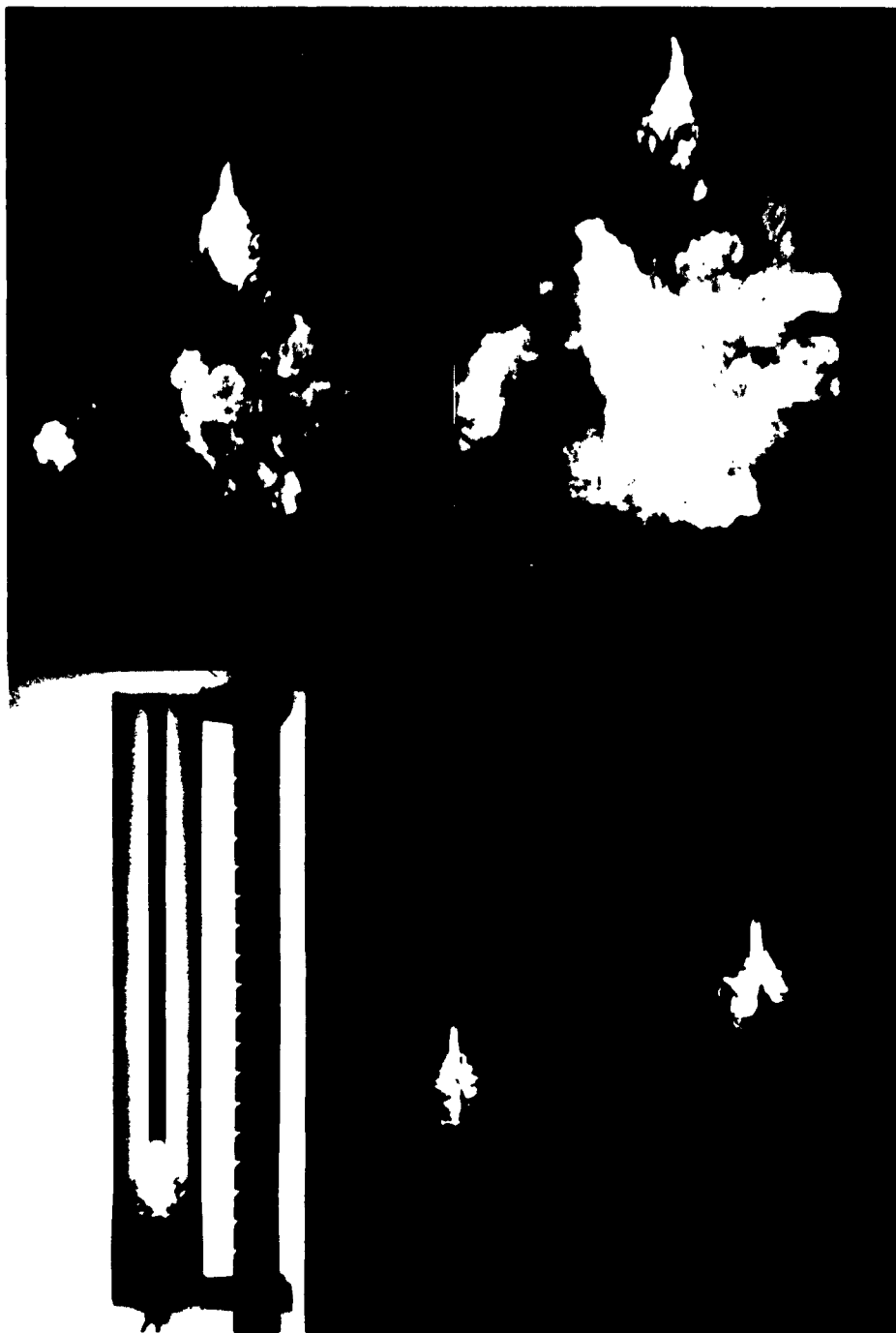


Fig 1 Propagation of Combustion in the Granular Mixture



Fig 2 Two Reaction Zone Profiles

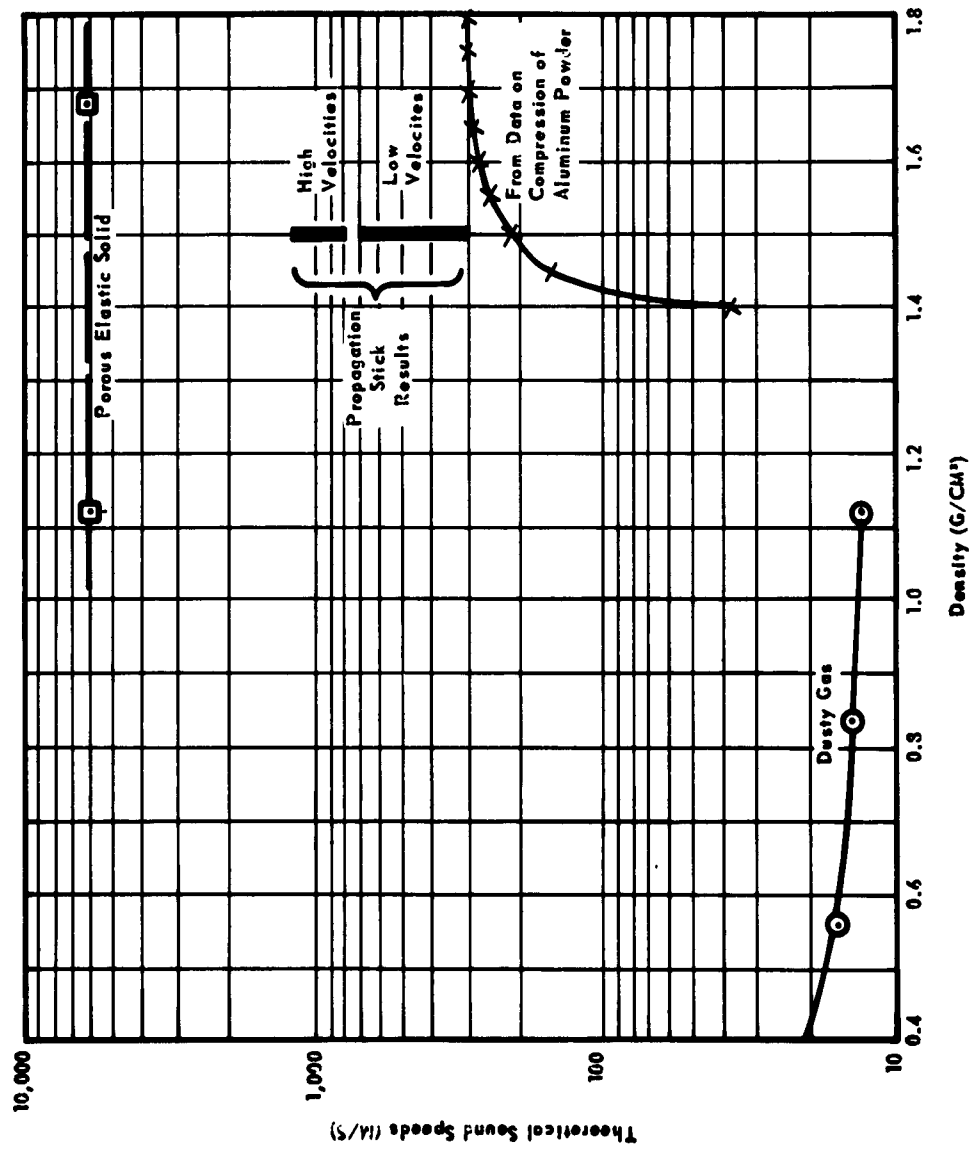


Fig 3 Sound Speed Considerations

## Appendix A

### DERIVATION OF JUMP CONDITIONS BY TWO APPROACHES

#### 1. Eulerian Coordinates

Let  $x_0(t)$  and  $x_1(t)$  be Eulerian coordinates of the front and back of moving element of mass which is our free body. Here  $dx$  is independent of time. For the observer fixed outside the flow, conservation of mass is then

$$\frac{d}{dt} \int_{x_0(t)}^{x_1(t)} \rho dx = 0 \quad \text{where} \quad x_0(t) = \int_0^t u(x, \tau) d\tau \quad (A1)$$

Apply Leibnitz rule (see last page)

$$\begin{aligned} \frac{d}{dt} \int_{x_0(t)}^{x_1(t)} \rho dx &= \int_{x_0}^{x_1} \frac{\partial \rho}{\partial t} dx + \dot{x}_1 \rho(x_1, t) - \dot{x}_0 \rho(x_0, t) = 0 \\ &= \int_{x_0}^{x_1} \frac{\partial \rho}{\partial t} dx + [\dot{x} \rho]_{x_0}^{x_1} = \int_{x_0}^{x_1} \frac{\partial \rho}{\partial t} dx + [u \rho]_{x_0}^{x_1} = 0 \quad (A2) \end{aligned}$$

Note that  $x_0$  and  $x_1$  in  $\int_{x_0}^{x_1} \frac{\partial \rho}{\partial t} dx$  can be any two fixed points chosen in the flow.

Consider a control surface moving at a velocity  $U$  with extremes  $x_0''(t)$  and  $x_1''(t)$ . Here again  $dx$  is independent of time

$$\begin{aligned} \left( \frac{d}{dt} \right)_U \int_{x_0''(t)}^{x_1''(t)} \rho dx &= \int_{x_0''}^{x_1''} \frac{\partial \rho}{\partial t} dx + \frac{dx_1''}{dt} \rho(x_1'', t) - \frac{dx_0''}{dt} \rho(x_0'', t) \\ &= \int_{x_0''}^{x_1''} \frac{\partial \rho}{\partial t} dx + U [\rho]_{x_0''}^{x_1''} \quad \text{for} \quad U = \frac{dx_1''}{dt} = \frac{dx_0''}{dt} \quad (A3) \end{aligned}$$

Now  $x_0''$  and  $x_1''$  are two positions in the flow and can be chosen coincident with  $x_0$  and  $x_1$ . The  $\frac{\partial \rho}{\partial t}$  in eq. A3 is the

same as that in eq. A2. and represents the rate seen by the observer outside the flow.

Combining eq. A2 and A3 by eliminating the integral with

$$\frac{d\rho}{dt} \text{ gives } \frac{d}{dt} \int_{x_0(t)}^{x_1(t)} \rho dx = \frac{d}{dt} \bigg|_u \int_{x_0''(t)}^{x_1''(t)} \rho dx + [(u-u)\rho]_{x_0}^{x_1} = 0 \quad (A4)$$

Note that  $x(t) = \int u(x,t) dt$  and  $x''(t) = Ut + \text{const.}$  Also  $x_0, x_1$  are fixed points coinciding with  $x_0'', x_1''$ .

$$\text{From eq. A4 } \frac{d}{dt} \bigg|_u \int_{x_0''(t)}^{x_1''(t)} \rho dx = - [(u-u)\rho]_{x_0}^{x_1}$$

Now if as the observer's control surface advances, the situation within is independent of time which is true for a detonation or stable deflagration, then

$$\frac{d}{dt} \bigg|_u \int_{x_0''(t)}^{x_1''(t)} \rho dx = 0 \quad \text{and} \quad [(u-u)\rho]_{x_0}^{x_1} = 0 \quad (A5)$$

This is the condition  $[\rho v]_{x_0}^{x_1} = 0$  which is the jump condition for conservation of mass. (eq 18 of report)

Now if we rewrite equation (A1) as (A1a)

$$\frac{d}{dt} \int_{x_0(t)}^{x_1(t)} F dx = 0 \quad (A1a)$$

Then all follows as previously leading to the corresponding

$$\text{jump conditions } [(u-u)F]_{x_0}^{x_1} = 0 \quad (A5a)$$

and if, we had used as our physical statement

$$\frac{d}{dt} \int_{x_0(t)}^{x_1(t)} F dx + [G]_{x_0}^{x_1} = 0 \quad (A1b)$$

then the jump condition is

$$\left[ (u - \bar{u}) F + G \right]_{x_0}^{x_1} = 0 \quad (A5b)$$

For conservation of momentum, the differential equation corresponding to eq Alb is

$$\frac{d}{dt} \int_{x_0(t)}^{x_1(t)} \rho u \, dx + \left[ p \right]_{x_0}^{x_1} = 0 \quad (A6)$$

The jump condition for momentum is therefore

$$\left[ (u - \bar{u}) \rho u + p \right]_{x_0}^{x_1} = 0 = \left[ \rho v^2 + \rho v \bar{u} + p \right]_{x_0}^{x_1}$$

Then using  $\mathcal{U}$  constant and conservation of mass there follows the jump condition for momentum

$$\left[ \rho v^2 + p \right]_{x_0}^{x_1} = 0 \quad (\text{eq 19 of report})$$

For conservation of energy the differential equation corresponding to eq Alb is

$$\frac{d}{dt} \int_{x_0(t)}^{x_1(t)} \rho \left( h + \frac{1}{2} u^2 - g \right) dx + \left[ \mathcal{U} p \right]_{x_0}^{x_1} = 0 \quad (A7)$$

The jump condition for energy is therefore

$$\left[ (u - \bar{u}) \rho \left( h + \frac{1}{2} u^2 - g \right) \right]_{x_0}^{x_1} + \left[ p \bar{u} \right]_{x_0}^{x_1} = 0$$

Using  $\mathcal{U}$  constant and the jump condition for mass and momentum this reduces to

$$\left[ h + \frac{1}{2} v^2 - g \right]_{x_0}^{x_1} = 0$$

$q$  is the heat added and is the negative of the enthalpy constant  $h_0$  related to formation. In the report  $h$  represented  $h - q$ , so that the jump condition equation 19 was

$$\left[ h + \frac{1}{2} v^2 \right]_{x_0}^{x_1} = 0$$

## II. Lagrangian Coordinates

In these coordinates, tags are associated with certain particle planes. Conservation mass holds for any integration limits in these coordinates.  $dx$  is a function of time  $\equiv \delta x$

$$\begin{aligned} \frac{D}{Dt} \int_{x_0}^{x_1} F(x,t) dx(t) & \quad \text{written} \quad \frac{D}{Dt} \int_{x_0}^{x_1} F \delta x \\ &= \frac{D}{Dt} \int_{x_0}^{x_1} \frac{F}{\rho} \rho \delta x = \int_{x_0}^{x_1} \frac{D}{Dt} \left\{ \frac{F}{\rho} \rho \delta x \right\} = \int_{x_0}^{x_1} \rho \delta x \frac{D}{Dt} \left( \frac{F}{\rho} \right) \text{ by } \frac{D}{Dt}(\rho \delta x) = 0 \\ &= \int_{x_0}^{x_1} \rho \delta x \left\{ \frac{1}{\rho} \frac{D}{Dt} (F) + (u \cdot \nabla) \frac{F}{\rho} \right\} = \int_{x_0}^{x_1} \delta x \left\{ \rho \frac{1}{\rho} \frac{D}{Dt} (F) + (\rho u \cdot \nabla) \frac{F}{\rho} \right\} \\ &= \int_{x_0}^{x_1} \delta x \left\{ \frac{\partial F}{\partial t} - \frac{F}{\rho} \frac{\partial \rho}{\partial t} + \nabla \cdot u F - \frac{F}{\rho} \nabla \cdot \rho u \right\} \end{aligned}$$

but  $\left\{ \frac{\partial \rho}{\partial t} + \nabla \cdot \rho u \right\} \delta x = 0$  by cons. of mass.

$$\frac{D}{Dt} \int_{x_0}^{x_1} F \delta x = \int_{x_0}^{x_1} \left( \frac{\partial F}{\partial t} + \nabla \cdot F u \right) \delta x = \int_{x_0}^{x_1} \frac{\partial F}{\partial t} \delta x + \left[ F u \right]_{x_0}^{x_1}$$

At a particular time  $t_0$ ,  $\int_{x_0}^{x_1} \frac{\partial F}{\partial t} \delta x = \int_{x_0}^{x_1} \frac{\partial F}{\partial t} dx$ ; where  $x \equiv x''$

Using eq A3 for this integral gives

$$\frac{D}{Dt} \int_{x_0}^{x_1} F \delta x = \frac{d}{dt} \bigg|_{t_0} \int_{x_0}^{x_1} F dx - 2 \left[ F \right]_{x_0}^{x_1} + \left[ F u \right]_{x_0}^{x_1}$$

This corresponds to eq. A4 and the jump condition follows in

similar fashion for  $\frac{D}{Dt} \int_{x_0}^{x_1} F \delta x = 0$  or with  $\left[ G \right]_{x_0}^{x_1}$  added.



# LEIBNITZ RULE

Let  $R$  be the rectangle defined by  $t_1 \leq t \leq t_2$   $a \leq x \leq b$   
 Let  $f(t, x)$  be bounded in  $R$  and integrable with respect to  $x$   
 for each value of  $t$ , and let  $\frac{\partial f}{\partial t}$  exist in  $R$  and also be  
 integrable in  $x$  for each value of  $t$ . Let  $\frac{\partial f}{\partial t}$  be  
 continuous for  $t = t_0$  uniformly as to  $x$  in  $\langle a, b \rangle$ . Let  $a(t)$   $b(t)$   
 be differentiable and  $f(t, x)$  continuous in  $x$  alone for each  
 value of  $t$  considered and for  $a(t) \leq x \leq b(t)$

$$\frac{d}{dt} \int_{a(t)}^{b(t)} f(t, x) dx = \int_a^b \frac{\partial f}{\partial t}(t, x) dx + f(t, b(t)) \frac{db(t)}{dt} - f(t, a(t)) \frac{da(t)}{dt}$$

here  $a$  and  $b$  are held constant, i.e., treated as regular definite integral between two fixed points.

## Appendix B

### SOLUTION OF THE EQUATIONS OF THE ONE PARAMETER HYDRODYNAMIC COMBUSTION THEORY

The equations originally presented in the OPHCT section of this report will be repeated here for convenience when required with the original numbers retained. Equations developed in this appendix have a letter B in their designation.

STEP 1 Solve eq 32, 33, 34, 35 for  $x_{Al}$ ,  $x_{Al_2O}$ ,  $x_{AlO}$ ,  $x_{O_2}$  in terms of  $p_2$ ,  $x_0$  and the functions of temperature a, b, c, d.

$$\frac{x_{AlO}}{x_{Al} x_0} = \frac{k_{AlO}}{k_0} p_2 = a(T_2) p_2 \quad (32)$$

$$\frac{x_{Al_2O}}{x_{Al}^2 x_0} = \frac{k_{Al_2O}}{k_0} p_2^2 = b(T_2) p_2^2 \quad (33)$$

$$\frac{1}{x_{Al}^2 x_0^3} = \frac{k_{Al_2O_3(c)}}{k_0^3} p_2^5 = c(T_2) p_2^5 \quad (34)$$

$$\frac{x_0}{x_{O_2}^{1/2}} = k_0 p_2^{-1/2} = d(T_2) p_2^{-1/2} \quad (35)$$

This gives

$$x_{Al} = c^{-1/2} p_2^{-1/2} x_0^{-1/2} = c^{-1/2} x_0^{1/2} = c^{-1/2} p_2^{-1} \quad (B1)$$

$$x_{a_{10}} = ac^{-\frac{1}{2}} p_2^{-\frac{3}{2}} x_0^{-\frac{1}{2}} = ac^{-\frac{1}{2}} S^3 x_0 = ac^{-\frac{1}{2}} S p_2^{-1} \quad (B2)$$

$$x_{a_{20}} = bc^{-1} p_2^{-3} x_0^{-2} = bc^{-1} S^6 x_0 = bc^{-1} S^4 p_2^{-1} \quad (B3)$$

$$x_{o_2} = d^{-2} p_2 x_0^2 = d^{-2} S^{-2} x_0 = d^{-2} S^{-4} p_2^{-1} \quad (B4)$$

We have used  $S = (p_2 x_0)^{-\frac{1}{2}}$  as a change in variable which eliminates fractional powers and gives a set linear in  $x_0 \sim p_2^{-1}$ . Note that  $x_{kr2}$ ,  $x_{a_{20_3}(c)}$  and  $N$  do not appear. These will be developed later.

**STEP 2** Eliminate  $x_{a_{20_3}(c)}$  by combining eq 28 and 29

$$x_{a_1} + x_{a_{10}} + 2x_{a_{20}} + 2x_{a_{20_3}(c)} = \frac{n_{a_1}}{N} \quad (28)$$

$$x_{a_{10}} + x_{a_{20}} + x_0 + 2x_{o_2} + 3x_{a_{20_3}} = \frac{4 n_{kr20_4}}{N} \quad (29)$$

$$3x_{a_1} + x_{a_{10}} + 4x_{a_{20}} - 2x_0 - 4x_{o_2} - \frac{3n_{a_1} - 8n_{kr20_4}}{N} = 0 \quad (B5)$$

Eliminate  $x_{kr2}$  by combining eq. 24 and 30.

$$1 = x_{a_1} + x_{a_{10}} + x_{a_{20}} + x_0 + x_{o_2} + x_{kr2} \quad (24)$$

$$x_{kr2} = \frac{n_{kr20_4}}{N} \quad (30)$$

$$x_{a_1} + x_{a_{10}} + x_{a_{20}} + x_0 + x_{o_2} + \frac{n_{kr20_4}}{N} = 1 \quad (B6)$$

Eliminate  $N$  by combining equations B5 and B6  
 Use  $f = 3n_{\text{Al}}' - 8n_{\text{KAlO}_4}'$  for convenience in writing.

$$(3g+f)x_{\text{Al}} + (g+f)x_{\text{Al}_2\text{O}_3} + (tg+f)x_{\text{Al}_2\text{O}_3} + (f-2g)x_{\text{O}} + (f-4g)x_{\text{O}_2} = f \quad (\text{B7})$$

STEP 3 - Substitute the results of Step 1 in equation B7 above.

This leads to the following equation in  $\zeta$  and  $x_0$

$$\frac{f}{x_0} = (3g+f)c^{-\frac{1}{2}}\zeta^5 + (g+f)ac^{-\frac{1}{2}}\zeta^3 + (tg+f)bc^{-1}\zeta^6 + (f-2g) + (f-4g)d^{-2}\zeta^{-2} \quad (\text{B8})$$

Dividing thru by  $f$  and writing  $\alpha = \frac{g}{f} = \frac{n_{\text{KAlO}_4}'}{3n_{\text{Al}}' - 8n_{\text{KAlO}_4}'}$

and using  $\zeta = (p_2 x_0)^{-\frac{1}{2}}$  or  $\frac{1}{x_0} = \zeta^2 p_2$  and solving for

$$p_2, \text{ we get } p_2 = \frac{(1+3\alpha)c^{-\frac{1}{2}}\zeta^3 + (1+\alpha)ac^{-\frac{1}{2}}\zeta + (1+4\alpha)bc^{-1}\zeta^4 + (1-2\alpha)\zeta^{-2} + (1-4\alpha)d^{-2}\zeta^{-4}}{\zeta^2} \quad (\text{B9})$$

\* Since eq B9 expresses  $p_2$  in terms of  $\zeta$ , it can be used in eq 21 to eliminate  $p_2$ . First, we modify equation 21.

$$h_2 - h_1 = \frac{1}{2}(p_2 - p_1)\left(\frac{1}{p_1} + \frac{1}{p_2}\right) \quad (21)$$

STEP 4 - Use eq 22 and 23 in eq 21 and multiply thru by  $\sum' x_i m_i$

$$\frac{1}{p_2} = \frac{R_m T_2}{p_2} \frac{1}{\sum' x_i m_i} + \frac{1}{p_{\text{Al}_2\text{O}_3}} \frac{x_{\text{Al}_2\text{O}_3} m_{\text{Al}_2\text{O}_3}}{\sum' x_i m_i} \quad (22)$$

$$h_2 = \left[ \sum' x_i (m_i h_{20i} + \int_{T_1}^{T_2} C_{p,i} dT) \right] / \sum' x_i m_i \quad (23)$$

$$\frac{1}{2}(p_2 - p_1) \left( \frac{\sum' x_i m_i}{p_1} + \frac{R_m T_2}{p_2} + \frac{\tau_{\text{Al}_2\text{O}_3} m_{\text{Al}_2\text{O}_3} x_{\text{Al}_2\text{O}_3}}{\sum' x_i m_i} \right) = \sum' x_i m_i h_{20i} + \sum' x_i \int_{T_1}^{T_2} C_{p,i} dT - \sum' x_i m_i h_1 = \sum' x_i (z_i - h_1 m_i) \quad (\text{B10})$$

where 
$$Z_i = H_{20i} + \int_T^{T_2} C_{p_i} dT$$

Now multiply both sides of B10 by  $p_2$  since  $p_2 x_i$  depends on  $\zeta$  only for  $x_{ae}$ ,  $x_{a20}$ ,  $x_{a2}$ ,  $x_{O_2}$  by eq B1, 2, 3, 7.

$$\frac{1}{2} (p_2 - p_1) \left( \frac{\sum' (x_i p_2) m_i}{\rho_1} + R_m T_2 + \frac{\tau p_2 m x}{a_{203}} \right) = \sum' (x_i p_2) (z_i - h_i m_i) \quad (B11)$$

Since eq. B9 gives  $p_2$  in terms of  $\zeta$  we lack only expressions for  $x_{KCl}$  and  $x_{a203}$  to be able to write an equation in  $\zeta$ .

STEP 5-Use eq 24 to provide an equation for  $x_{KCl}$ , multiply by  $p_2$  and insert eq. B1, B2, B3, and B9 to obtain the equation for  $p_2 x_{KCl}$

$$p_2 x_{KCl} = 4\alpha b c^{-1} \zeta^{-4} + 3\alpha c^{-\frac{1}{2}} \zeta^{-3} + \alpha a c^{-\frac{1}{2}} \zeta^{-1} - 2\alpha \zeta^{-2} - 4\alpha d^{-2} \zeta^{-4} \quad (B12)$$

To obtain  $p_2 x_{a203}$ , solve for  $x_{a203}$  by combining eq 28 and 29. Use eq B6 to replace  $N$ . Finally multiply by  $p_2$  and use eq B9

This results in 
$$x_{a203} = n + (1-n) x_{ae} - n x_{a20} - (1+n) x_{O_2} + (1-n) x_{a20} - (1+n) x_O \quad (B13)$$

$$p_2 x_{a203} = (1+4n\alpha) b c^{-1} \zeta^{-4} + (1+3n\alpha) c^{-\frac{1}{2}} \zeta^{-3} + n\alpha a c^{-\frac{1}{2}} \zeta^{-1} - (1+2n\alpha) \zeta^{-2} - (2+4n\alpha) d^{-2} \zeta^{-4} \quad (B14)$$

$$n = \left[ (4n^0_{KClO_4} - n^0_{ae}) / (n^0_{KClO_4}) \right]$$

STEP 6-To obtain the polynomial in  $\zeta$ , we substitute B12, B14,

B1, B2, B3, B4 and B9 in B11, and collect coefficients of each power of  $\zeta$ . The equation is

$$\begin{aligned} & \{ A_0 \zeta^4 + B_0 \zeta^3 + C_0 \zeta + D_0 \zeta^{-2} + E_0 \zeta^{-4} - p_1 \} \times \\ & \{ A_m \zeta^4 + B_m \zeta^3 + C_m \zeta + D_m \zeta^{-2} + E_m \zeta^{-4} + R_m T_2 \} = \\ & \{ A_z \zeta^4 + B_z \zeta^3 + C_z \zeta + D_z \zeta^{-2} + E_z \zeta^{-4} \} \quad (B15) \end{aligned}$$

where  $A_0 = \frac{1}{2} (1+4\alpha) b c^{-1}$   $B_0 = \frac{1}{2} (1+3\alpha) c^{-\frac{1}{2}}$   $C_0 = \frac{1}{2} (1+\alpha) a c^{-\frac{1}{2}}$

$$D_0 = \frac{1}{2} (1-2\alpha) \quad E_0 = \frac{1}{2} (1+4\alpha) d^{-2}$$

$$A_m = \frac{m_{al_2O}}{\rho_1} b c^{-1} + \frac{m_{KCl}}{\rho_1} 4\alpha b c^{-1} + \left(\tau + \frac{1}{\rho_1}\right) m_{al_2O_3} (1+4n\alpha) b c^{-1}$$

$$B_m = \frac{m_{al}}{\rho_1} c^{-\frac{1}{2}} + \frac{m_{KCl}}{\rho_1} 3\alpha c^{-\frac{1}{2}} + \left(\tau + \frac{1}{\rho_1}\right) m_{al_2O_3} (1+3n\alpha) c^{-\frac{1}{2}}$$

$$C_m = \frac{m_{alO}}{\rho_1} a c^{-\frac{1}{2}} + \frac{m_{KCl}}{\rho_1} \alpha a c^{-\frac{1}{2}} + \left(\tau + \frac{1}{\rho_1}\right) m_{al_2O_3} (n\alpha a c^{-\frac{1}{2}})$$

$$D_m = \frac{m_O}{\rho_1} - \frac{m_{KCl}}{\rho_1} 2\alpha - \left(\tau + \frac{1}{\rho_1}\right) m_{al_2O_3} (1+2n\alpha)$$

$$E_m = \frac{m_{O_2}}{\rho_1} d^{-2} - \frac{m_{KCl}}{\rho_1} 4\alpha d^{-2} - \left(\tau + \frac{1}{\rho_1}\right) m_{al_2O_3} (2+4n\alpha) d^{-2}$$

$A_2$   $B_2$   $C_2$   $D_2$   $E_2$  are obtained from

$A_m$   $B_m$   $C_m$   $D_m$   $E_m$  respectively by

replacing each mass/density quotient by the corresponding  $z_i - h_i m_i$ .

Thus

$$A_2 = (z_{al_2O} - h_1 m_{al_2O}) b c^{-1} + (z_{KCl} - h_1 m_{KCl}) 4\alpha b c^{-1} \\ + (z_{al_2O_3} - h_1 m_{al_2O_3}) (1+4n\alpha) b c^{-1}$$

The roots of eq. B15 are more easily found if it is put in the standard polynomial form. To achieve this, multiply through by  $S^8$ , evaluate the product on the left side, transpose and collect coefficients of the same powers of  $S$ . This results in

$$\begin{aligned} & \{A_0 S^8 + B_0 S^7 + C_0 S^6 + D_0 S^5 + E_0 - p_1 S^4\} \times \\ & \{A_m S^8 + B_m S^7 + C_m S^6 + D_m S^5 + E_m + R_m T_2 S^4\} = \\ & \{A_2 S^{12} + B_2 S^{11} + C_2 S^{10} + D_2 S^9 + E_2 S^8\} \end{aligned}$$

which leads to the following

$$\begin{aligned} & A_m A_0 S^{16} + (A_m B_0 + B_m A_0) S^{15} + B_m B_0 S^{14} \\ & + (A_m C_0 + C_m A_0) S^{13} + (B_m C_0 + C_m B_0 + R_m T_2 A_0 - A_m p_1 - A_2) S^{12} \\ & + (R_m T_2 B_0 - B_m p_1 - B_2) S^{11} + (A_m D_0 + C_m C_0 + D_m A_0) S^{10} \\ & + (B_m D_0 + D_m B_0 + R_m T_2 C_0 - C_m p_1 - C_2) S^9 \\ & + (A_m E_0 + E_m A_0 - R_m T_2 p_1) S^8 \\ & + (B_m E_0 + C_m D_0 + D_m C_0 + E_m B_0) S^7 \\ & + (R_m T_2 D_0 - D_m p_1 - D_2) S^6 + (C_m E_0 + E_m C_0) S^5 \\ & + (D_m D_0 + R_m T_2 E_0 - E_m p_1 - E_2) S^4 \\ & + (D_m E_0 + E_m D_0) S^2 + E_m E_0 = 0 \quad (B16) \end{aligned}$$

Equation B16 is the required polynomial in  $\zeta$  which combines all 10 equations and avoids the need for iterative solutions of the set. Once  $\zeta$  is found, the various equations are used to obtain for a particular  $T_2$  the corresponding values of  $p_2$ ,  $\rho_2$ ,  $x_i$ . Then  $\rho_2$  follows from eq. 22. The velocities  $u_2$ ,  $u$  are obtained from the jump conditions for mass and momentum.



# INITIAL DISTRIBUTION LIST

	Copy No.
Commanding General Hq, US Army Munition Command Dover, New Jersey	1-2
Commanding Officer Army Research Office (Durham) Durham, North Carolina	3-4
Commanding Officer Ballistics Research Laboratory Aberdeen, Maryland	
ATTN: Dr. F. A. Allison	5
Dr. R. Eichelberger	6
Technical Library	7
ASTIA	8-27
Commander Naval Ordnance Laboratory Silver Springs, Maryland	
ATTN: Dr. Sternberg	28
Dr. Drimmer	29
Los Alamos Scientific Laboratory Los Alamos, New Mexico	
ATTN: Dr. C. Mader	30
Dr. W. W. Wood	31
Bureau of Mines Division of Explosives Technology 4800 Forbes Avenue Pittsburgh, Pennsylvania	
ATTN: Dr. H. M. Cassel	32-33
Lawrence Radiation Laboratory Livermore, California	
ATTN: Dr. R. Duff	34-35
Sandia Corporation Division 5133 Albuquerque, New Mexico	
ATTN: Dr. Glenn E. Seay	36-37

**Copy No.**

<b>Rohm &amp; Hass Company Redstone Arsenal Research Division Huntsville, Alabama</b>	<b>38-39</b>
<b>Commander Naval Ordnance Testing Station China Lake, California ATTN: Dr. H. J. Gryting</b>	<b>40-41</b>
<b>Brown University Division of Engineering 182 George Street Providence 12, Rhode Island ATTN: Dr. B. T. Chu</b>	<b>42-43</b>
<b>Princeton University Dept of Aeronautical Engineering Princeton, New Jersey ATTN: Dr. I. Glassman</b>	<b>44</b>
<b>Stanford Research Institute Poulter Laboratories Menlo Park, California ATTN: Dr. M. Evans</b>	<b>45</b>
<b>Courant Institute of Mathematical Sciences New York University Washington Square 3, New York ATTN: Dr. J. Keller</b>	<b>46</b>
<b>E. I. duPont deNemours and Co. Eastern Laboratory Gibbstown, New Jersey ATTN: Dr. C. Davis</b>	<b>47</b>
<b>Geophysics Corporation of America 700 Commonwealth Avenue Boston 15, Massachusetts ATTN: Mr. A. W. Berger</b>	<b>48</b>

	Copy No.
Johns Hopkins University Department of Chemical Engineering Baltimore 18, Maryland ATTN: Dr. H. E. Hoelscher	49
The Pennsylvania State University Department of Fuel Technology University Park, Pennsylvania ATTN: Dr. J. Seery	50
Lehigh University Bethlehem, Pennsylvania ATTN: Dr. R. J. Emrich	51
General Electric Company Missile and Ordnance Systems Department 3198 Chestnut Street Philadelphia 4, Pennsylvania ATTN: Dr. Partick J. Friel	52
Atlantic Research Corporation Alexandria, Virginia ATTN: Dr. A. Macek	53
Hercules Powder Company Magna, Utah ATTN: Mr. D. H. Black	54
Rensselaer Polytechnic Research Division Rensselaer Polytechnic Institute Troy, New York ATTN: Dr. S. Katz	55
Applied Physics Laboratory Johns Hopkins University Silver Springs, Md. ATTN: Mr. C. Dunkel	56
Stevens Institute of Technology Hoboken, New Jersey ATTN: Dr. S. Lukasik	57

Copy No.

Armed Services Technical Information Agency  
Arlington Hall Station  
Arlington 12, Virginia

58-67

Accession No. _____ AD _____ Picatinny Arsenal, Dover, N. J.  <b>THE COMBUSTION OF A GRANULAR MIXTURE OF POTASSIUM PERCHLORATE AND ALUMINUM CONSIDERED AS EITHER A DEFLAGRATION OR A DETONATION</b> Joseph Hershkowitz  Technical Report 3063, February 1963, 61 pp, graphs, photographs, tables. Unclassified report from the Engineering Sciences Laboratory of the Feltman Research Laboratories  The combustion front in a column of a granular mixture of potassium perchlorate and aluminum has been observed to propagate stably at either a low speed  (over)	1. Combustion 2. Aluminized explosives - Combustion  1. Hershkowitz, Joseph <b>UNITERMS</b>  Combustion Potassium perchlorate Aluminum Detonation Deflagration Hershkowitz, J.	Accession No. _____ AD _____ Picatinny Arsenal, Dover, N. J.  <b>THE COMBUSTION OF A GRANULAR MIXTURE OF POTASSIUM PERCHLORATE AND ALUMINUM CONSIDERED AS EITHER A DEFLAGRATION OR A DETONATION</b> Joseph Hershkowitz  Technical Report 3063, February 1963, 61 pp, graphs, photographs, tables. Unclassified report from the Engineering Sciences Laboratory of the Feltman Research Laboratories  The combustion front in a column of a granular mixture of potassium perchlorate and aluminum has been observed to propagate stably at either a low speed  (over)	1. Combustion 2. Aluminized explosives - Combustion  1. Hershkowitz, Joseph <b>UNITERMS</b>  Combustion Potassium perchlorate Aluminum Detonation Deflagration Hershkowitz, J.	Accession No. _____ AD _____ Picatinny Arsenal, Dover, N. J.  <b>THE COMBUSTION OF A GRANULAR MIXTURE OF POTASSIUM PERCHLORATE AND ALUMINUM CONSIDERED AS EITHER A DEFLAGRATION OR A DETONATION</b> Joseph Hershkowitz  Technical Report 3063, February 1963, 61 pp, graphs, photographs, tables. Unclassified report from the Engineering Sciences Laboratory of the Feltman Research Laboratories  The combustion front in a column of a granular mixture of potassium perchlorate and aluminum has been observed to propagate stably at either a low speed  (over)	1. Combustion 2. Aluminized explosives - Combustion  1. Hershkowitz, Joseph <b>UNITERMS</b>  Combustion Potassium perchlorate Aluminum Detonation Deflagration Hershkowitz, J.	Accession No. _____ AD _____ Picatinny Arsenal, Dover, N. J.  <b>THE COMBUSTION OF A GRANULAR MIXTURE OF POTASSIUM PERCHLORATE AND ALUMINUM CONSIDERED AS EITHER A DEFLAGRATION OR A DETONATION</b> Joseph Hershkowitz  Technical Report 3063, February 1963, 61 pp, graphs, photographs, tables. Unclassified report from the Engineering Sciences Laboratory of the Feltman Research Laboratories  The combustion front in a column of a granular mixture of potassium perchlorate and aluminum has been observed to propagate stably at either a low speed  (over)	1. Combustion 2. Aluminized explosives - Combustion  1. Hershkowitz, Joseph <b>UNITERMS</b>  Combustion Potassium perchlorate Aluminum Detonation Deflagration Hershkowitz, J.
---	--	---	--	---	--	---	--

(300 m/s) with a short reaction zone (2 cm), or a higher one (900 m/s) with an elongated reaction zone (8 cm), and with an occasional rapid transition between them. Calculations are made to categorize the observed phenomena as those of either a deflagration or a detonation. Calculating the penetration depth from the front into the mixture for diffusion of molecules, thermal energy, and radiant energy shows that these deflagrative mechanisms have negligible effect at the rates observed and suggests that deflagration would proceed at less than 0.3 m/s. A calculation of the deflagration branch of the Hugoniot by a parametric technique also shows that only rates of the order of 0.1 m/s exist for deflagrations. The calculated sound speed for the unreacted granular mixture is less than 300 m/s. The hypotheses of a simple deflagration and of a deflagration following a precompression shock are rejected.

The RUBY computer program calculated a detonation velocity for the mixture of 4600 m/s. This would be reduced by the observed lateral rarefaction in the reaction zone. Further experiments and theoretical studies to establish the details of the detonative nature of the phenomena are outlined.

(300 m/s) with a short reaction zone (2 cm), or a higher one (900 m/s) with an elongated reaction zone (8 cm), and with an occasional rapid transition between them. Calculations are made to categorize the observed phenomena as those of either a deflagration or a detonation. Calculating the penetration depth from the front into the mixture for diffusion of molecules, thermal energy, and radiant energy shows that these deflagrative mechanisms have negligible effect at the rates observed and suggests that deflagration would proceed at less than 0.3 m/s. A calculation of the deflagration branch of the Hugoniot by a parametric technique also shows that only rates of the order of 0.1 m/s exist for deflagrations. The calculated sound speed for the unreacted granular mixture is less than 300 m/s. The hypotheses of a simple deflagration and of a deflagration following a precompression shock are rejected.

The RUBY computer program calculated a detonation velocity for the mixture of 4600 m/s. This would be reduced by the observed lateral rarefaction in the reaction zone. Further experiments and theoretical studies to establish the details of the detonative nature of the phenomena are outlined.

(300 m/s) with a short reaction zone (2 cm), or a higher one (900 m/s) with an elongated reaction zone (8 cm), and with an occasional rapid transition between them. Calculations are made to categorize the observed phenomena as those of either a deflagration or a detonation.

Calculating the penetration depth from the front into the mixture for diffusion of molecules, thermal energy, and radiant energy shows that these deflagrative mechanisms have negligible effect at the rates observed and suggests that deflagration would proceed at less than 0.3 m/s. A calculation of the deflagration branch of the Hugoniot by a parametric technique also shows that only rates of the order of 0.1 m/s exist for deflagrations. The calculated sound speed for the unreacted granular mixture is less than 300 m/s. The hypotheses of a simple deflagration and of a deflagration following a precompression shock are rejected.

The RUBY computer program calculated a detonation velocity for the mixture of 4600 m/s. This would be reduced by the observed lateral rarefaction in the reaction zone. Further experiments and theoretical studies to establish the details of the detonative nature of the phenomena are outlined.

(300 m/s) with a short reaction zone (2 cm), or a higher one (900 m/s) with an elongated reaction zone (8 cm), and with an occasional rapid transition between them. Calculations are made to categorize the observed phenomena as those of either a deflagration or a detonation.

Calculating the penetration depth from the front into the mixture for diffusion of molecules, thermal energy, and radiant energy shows that these deflagrative mechanisms have negligible effect at the rates observed and suggests that deflagration would proceed at less than 0.3 m/s. A calculation of the deflagration branch of the Hugoniot by a parametric technique also shows that only rates of the order of 0.1 m/s exist for deflagrations. The calculated sound speed for the unreacted granular mixture is less than 300 m/s. The hypotheses of a simple deflagration and of a deflagration following a precompression shock are rejected.

The RUBY computer program calculated a detonation velocity for the mixture of 4600 m/s. This would be reduced by the observed lateral rarefaction in the reaction zone. Further experiments and theoretical studies to establish the details of the detonative nature of the phenomena are outlined.

Accession No. \_\_\_\_\_ AD \_\_\_\_\_  
Picatinny Arsenal, Dover, N. J.

**THE COMBUSTION OF A GRANULAR MIXTURE OF  
POTASSIUM PERCHLORATE AND ALUMINUM CON-  
SIDERED AS EITHER A DEFLAGRATION OR A  
DETONATION**

Joseph Hershkowitz

Technical Report 3063, February 1963, 61 pp, graphs,  
photographs, tables. Unclassified report from the Engi-  
neering Sciences Laboratory of the Feltman Research  
Laboratories

The combustion front in a column of a granular mixture  
of potassium perchlorate and aluminum has been ob-  
served to propagate stably at either a low speed

(over)

1. Combustion
2. Aluminized explosives  
    - Combustion

I. Hershkowitz, Joseph

**UNITERMS**

Combustion  
Potassium perchlorate  
Aluminum  
Detonation  
Deflagration  
Hershkowitz, J.

Accession No. \_\_\_\_\_ AD \_\_\_\_\_  
Picatinny Arsenal, Dover, N. J.

**THE COMBUSTION OF A GRANULAR MIXTURE OF  
POTASSIUM PERCHLORATE AND ALUMINUM CON-  
SIDERED AS EITHER A DEFLAGRATION OR A  
DETONATION**

Joseph Hershkowitz

Technical Report 3063, February 1963, 61 pp, graphs,  
photographs, tables. Unclassified report from the Engi-  
neering Sciences Laboratory of the Feltman Research  
Laboratories

The combustion front in a column of a granular mixture  
of potassium perchlorate and aluminum has been ob-  
served to propagate stably at either a low speed

(over)

1. Combustion
2. Aluminized explosives  
    - Combustion

I. Hershkowitz, Joseph

**UNITERMS**

Combustion  
Potassium perchlorate  
Aluminum  
Detonation  
Deflagration  
Hershkowitz, J.

Accession No. \_\_\_\_\_ AD \_\_\_\_\_  
Picatinny Arsenal, Dover, N. J.

**THE COMBUSTION OF A GRANULAR MIXTURE OF  
POTASSIUM PERCHLORATE AND ALUMINUM CON-  
SIDERED AS EITHER A DEFLAGRATION OR A  
DETONATION**

Joseph Hershkowitz

Technical Report 3063, February 1963, 61 pp, graphs,  
photographs, tables. Unclassified report from the Engi-  
neering Sciences Laboratory of the Feltman Research  
Laboratories

The combustion front in a column of a granular mixture  
of potassium perchlorate and aluminum has been ob-  
served to propagate stably at either a low speed

(over)

1. Combustion
2. Aluminized explosives  
    - Combustion

I. Hershkowitz, Joseph

**UNITERMS**

Combustion  
Potassium perchlorate  
Aluminum  
Detonation  
Deflagration  
Hershkowitz, J.

Accession No. \_\_\_\_\_ AD \_\_\_\_\_  
Picatinny Arsenal, Dover, N. J.

**THE COMBUSTION OF A GRANULAR MIXTURE OF  
POTASSIUM PERCHLORATE AND ALUMINUM CON-  
SIDERED AS EITHER A DEFLAGRATION OR A  
DETONATION**

Joseph Hershkowitz

Technical Report 3063, February 1963, 61 pp, graphs,  
photographs, tables. Unclassified report from the Engi-  
neering Sciences Laboratory of the Feltman Research  
Laboratories

The combustion front in a column of a granular mixture  
of potassium perchlorate and aluminum has been ob-  
served to propagate stably at either a low speed

(over)

1. Combustion
2. Aluminized explosives  
    - Combustion

I. Hershkowitz, Joseph

**UNITERMS**

Combustion  
Potassium perchlorate  
Aluminum  
Detonation  
Deflagration  
Hershkowitz, J.

(300 m/s) with a short reaction zone (2 cm), or a higher one (900 m/s) with an elongated reaction zone (8 cm), and with an occasional rapid transition between them. Calculations are made to categorize the observed phenomena as those of either a deflagration or a detonation.

Calculating the penetration depth from the front into the mixture for diffusion of molecules, thermal energy, and radiant energy shows that these deflagrative mechanisms have negligible effect at the rates observed and suggests that deflagration would proceed at less than 0.3 m/s. A calculation of the deflagration branch of the Hugoniot by a parametric technique also shows that only rates of the order of 0.1 m/s exist for deflagrations. The calculated sound speed for the unreacted granular mixture is less than 300 m/s. The hypotheses of a simple deflagration and of a deflagration following a precompression shock are rejected.

The RUBY computer program calculated a detonation velocity for the mixture of 4600 m/s. This would be reduced by the observed lateral rarefaction in the reaction zone. Further experiments and theoretical studies to establish the details of the detonative nature of the phenomena are outlined.

(300 m/s) with a short reaction zone (2 cm), or a higher one (900 m/s) with an elongated reaction zone (8 cm), and with an occasional rapid transition between them. Calculations are made to categorize the observed phenomena as those of either a deflagration or a detonation.

Calculating the penetration depth from the front into the mixture for diffusion of molecules, thermal energy, and radiant energy shows that these deflagrative mechanisms have negligible effect at the rates observed and suggests that deflagration would proceed at less than 0.3 m/s. A calculation of the deflagration branch of the Hugoniot by a parametric technique also shows that only rates of the order of 0.1 m/s exist for deflagrations. The calculated sound speed for the unreacted granular mixture is less than 300 m/s. The hypotheses of a simple deflagration and of a deflagration following a precompression shock are rejected.

The RUBY computer program calculated a detonation velocity for the mixture of 4600 m/s. This would be reduced by the observed lateral rarefaction in the reaction zone. Further experiments and theoretical studies to establish the details of the detonative nature of the phenomena are outlined.

(300 m/s) with a short reaction zone (2 cm), or a higher one (900 m/s) with an elongated reaction zone (8 cm), and with an occasional rapid transition between them. Calculations are made to categorize the observed phenomena as those of either a deflagration or a detonation.

Calculating the penetration depth from the front into the mixture for diffusion of molecules, thermal energy, and radiant energy shows that these deflagrative mechanisms have negligible effect at the rates observed and suggests that deflagration would proceed at less than 0.3 m/s. A calculation of the deflagration branch of the Hugoniot by a parametric technique also shows that only rates of the order of 0.1 m/s exist for deflagrations. The calculated sound speed for the unreacted granular mixture is less than 300 m/s. The hypotheses of a simple deflagration and of a deflagration following a precompression shock are rejected.

The RUBY computer program calculated a detonation velocity for the mixture of 4600 m/s. This would be reduced by the observed lateral rarefaction in the reaction zone. Further experiments and theoretical studies to establish the details of the detonative nature of the phenomena are outlined.

(300 m/s) with a short reaction zone (2 cm), or a higher one (900 m/s) with an elongated reaction zone (8 cm), and with an occasional rapid transition between them. Calculations are made to categorize the observed phenomena as those of either a deflagration or a detonation.

Calculating the penetration depth from the front into the mixture for diffusion of molecules, thermal energy, and radiant energy shows that these deflagrative mechanisms have negligible effect at the rates observed and suggests that deflagration would proceed at less than 0.3 m/s. A calculation of the deflagration branch of the Hugoniot by a parametric technique also shows that only rates of the order of 0.1 m/s exist for deflagrations. The calculated sound speed for the unreacted granular mixture is less than 300 m/s. The hypotheses of a simple deflagration and of a deflagration following a precompression shock are rejected.

The RUBY computer program calculated a detonation velocity for the mixture of 4600 m/s. This would be reduced by the observed lateral rarefaction in the reaction zone. Further experiments and theoretical studies to establish the details of the detonative nature of the phenomena are outlined.



Accession No. \_\_\_\_\_ AD \_\_\_\_\_  
Picatinny Arsenal, Dover, N. J.

THE COMBUSTION OF A GRANULAR MIXTURE OF  
POTASSIUM PERCHLORATE AND ALUMINUM CON-  
SIDERED AS EITHER A DEFLAGRATION OR A  
DETONATION

Joseph Hershkowitz

Technical Report 3063, February 1963, 61 pp, graphs,  
photographs, tables. Unclassified report from the Engi-  
neering Sciences Laboratory of the Feltman Research  
Laboratories

The combustion front in a column of a granular mixture  
of potassium perchlorate and aluminum has been ob-  
served to propagate stably at either a low speed

(over)

1. Combustion  
2. Aluminized explosives  
- Combustion

1. Hershkowitz, Joseph  
UNITERMS

Combustion  
Potassium perchlorate  
Aluminum  
Detonation  
Deflagration  
Hershkowitz, J.

Accession No. \_\_\_\_\_ AD \_\_\_\_\_  
Picatinny Arsenal, Dover, N. J.

THE COMBUSTION OF A GRANULAR MIXTURE OF  
POTASSIUM PERCHLORATE AND ALUMINUM CON-  
SIDERED AS EITHER A DEFLAGRATION OR A  
DETONATION

Joseph Hershkowitz

Technical Report 3063, February 1963, 61 pp, graphs,  
photographs, tables. Unclassified report from the Engi-  
neering Sciences Laboratory of the Feltman Research  
Laboratories

The combustion front in a column of a granular mixture  
of potassium perchlorate and aluminum has been ob-  
served to propagate stably at either a low speed

(over)

1. Combustion  
2. Aluminized explosives  
- Combustion

1. Hershkowitz, Joseph  
UNITERMS

Combustion  
Potassium perchlorate  
Aluminum  
Detonation  
Deflagration  
Hershkowitz, J.

Accession No. \_\_\_\_\_ AD \_\_\_\_\_  
Picatinny Arsenal, Dover, N. J.

THE COMBUSTION OF A GRANULAR MIXTURE OF  
POTASSIUM PERCHLORATE AND ALUMINUM CON-  
SIDERED AS EITHER A DEFLAGRATION OR A  
DETONATION

Joseph Hershkowitz

Technical Report 3063, February 1963, 61 pp, graphs,  
photographs, tables. Unclassified report from the Engi-  
neering Sciences Laboratory of the Feltman Research  
Laboratories

The combustion front in a column of a granular mixture  
of potassium perchlorate and aluminum has been ob-  
served to propagate stably at either a low speed

(over)

1. Combustion  
2. Aluminized explosives  
- Combustion

1. Hershkowitz, Joseph  
UNITERMS

Combustion  
Potassium perchlorate  
Aluminum  
Detonation  
Deflagration  
Hershkowitz, J.

Accession No. \_\_\_\_\_ AD \_\_\_\_\_  
Picatinny Arsenal, Dover, N. J.

THE COMBUSTION OF A GRANULAR MIXTURE OF  
POTASSIUM PERCHLORATE AND ALUMINUM CON-  
SIDERED AS EITHER A DEFLAGRATION OR A  
DETONATION

Joseph Hershkowitz

Technical Report 3063, February 1963, 61 pp, graphs,  
photographs, tables. Unclassified report from the Engi-  
neering Sciences Laboratory of the Feltman Research  
Laboratories

The combustion front in a column of a granular mixture  
of potassium perchlorate and aluminum has been ob-  
served to propagate stably at either a low speed

(over)

1. Combustion  
2. Aluminized explosives  
- Combustion

1. Hershkowitz, Joseph  
UNITERMS

Combustion  
Potassium perchlorate  
Aluminum  
Detonation  
Deflagration  
Hershkowitz, J.

(300 m/s) with a short reaction zone (2 cm), or a higher one (900 m/s) with an elongated reaction zone (8 cm), and with an occasional rapid transition between them. Calculations are made to categorize the observed phenomena as those of either a deflagration or a detonation.

Calculating the penetration depth from the front into the mixture for diffusion of molecules, thermal energy, and radiant energy shows that these deflagrative mechanisms have negligible effect at the rates observed and suggests that deflagration would proceed at less than 0.3 m/s. A calculation of the deflagration branch of the Hugoniot by a parametric technique also shows that only rates of the order of 0.1 m/s exist for deflagrations. The calculated sound speed for the unreacted granular mixture is less than 300 m/s. The hypotheses of a simple deflagration and of a deflagration following a precompression shock are rejected.

The RUBY computer program calculated a detonation velocity for the mixture of 4600 m/s. This would be reduced by the observed lateral rarefaction in the reaction zone. Further experiments and theoretical studies to establish the details of the detonative nature of the phenomena are outlined.

(300 m/s) with a short reaction zone (2 cm), or a higher one (900 m/s) with an elongated reaction zone (8 cm), and with an occasional rapid transition between them. Calculations are made to categorize the observed phenomena as those of either a deflagration or a detonation.

Calculating the penetration depth from the front into the mixture for diffusion of molecules, thermal energy, and radiant energy shows that these deflagrative mechanisms have negligible effect at the rates observed and suggests that deflagration would proceed at less than 0.3 m/s. A calculation of the deflagration branch of the Hugoniot by a parametric technique also shows that only rates of the order of 0.1 m/s exist for deflagrations. The calculated sound speed for the unreacted granular mixture is less than 300 m/s. The hypotheses of a simple deflagration and of a deflagration following a precompression shock are rejected.

The RUBY computer program calculated a detonation velocity for the mixture of 4600 m/s. This would be reduced by the observed lateral rarefaction in the reaction zone. Further experiments and theoretical studies to establish the details of the detonative nature of the phenomena are outlined.

(300 m/s) with a short reaction zone (2 cm), or a higher one (900 m/s) with an elongated reaction zone (8 cm), and with an occasional rapid transition between them. Calculations are made to categorize the observed phenomena as those of either a deflagration or a detonation.

Calculating the penetration depth from the front into the mixture for diffusion of molecules, thermal energy, and radiant energy shows that these deflagrative mechanisms have negligible effect at the rates observed and suggests that deflagration would proceed at less than 0.3 m/s. A calculation of the deflagration branch of the Hugoniot by a parametric technique also shows that only rates of the order of 0.1 m/s exist for deflagrations. The calculated sound speed for the unreacted granular mixture is less than 300 m/s. The hypotheses of a simple deflagration and of a deflagration following a precompression shock are rejected.

The RUBY computer program calculated a detonation velocity for the mixture of 4600 m/s. This would be reduced by the observed lateral rarefaction in the reaction zone. Further experiments and theoretical studies to establish the details of the detonative nature of the phenomena are outlined.

(300 m/s) with a short reaction zone (2 cm), or a higher one (900 m/s) with an elongated reaction zone (8 cm), and with an occasional rapid transition between them. Calculations are made to categorize the observed phenomena as those of either a deflagration or a detonation.

Calculating the penetration depth from the front into the mixture for diffusion of molecules, thermal energy, and radiant energy shows that these deflagrative mechanisms have negligible effect at the rates observed and suggests that deflagration would proceed at less than 0.3 m/s. A calculation of the deflagration branch of the Hugoniot by a parametric technique also shows that only rates of the order of 0.1 m/s exist for deflagrations. The calculated sound speed for the unreacted granular mixture is less than 300 m/s. The hypotheses of a simple deflagration and of a deflagration following a precompression shock are rejected.

The RUBY computer program calculated a detonation velocity for the mixture of 4600 m/s. This would be reduced by the observed lateral rarefaction in the reaction zone. Further experiments and theoretical studies to establish the details of the detonative nature of the phenomena are outlined.